Electromagnetic (time like and space like) baryon transition form factors

Teresa Peña (IST-ULisboa)
and
Gilberto Ramalho, LFTC,
Universidade Cruzeiro do Sul,
Brasil

Kandisky “Circles in a circle” (1923)

Timelike: $Q^2<0$	Spacelike: $Q^2>0$

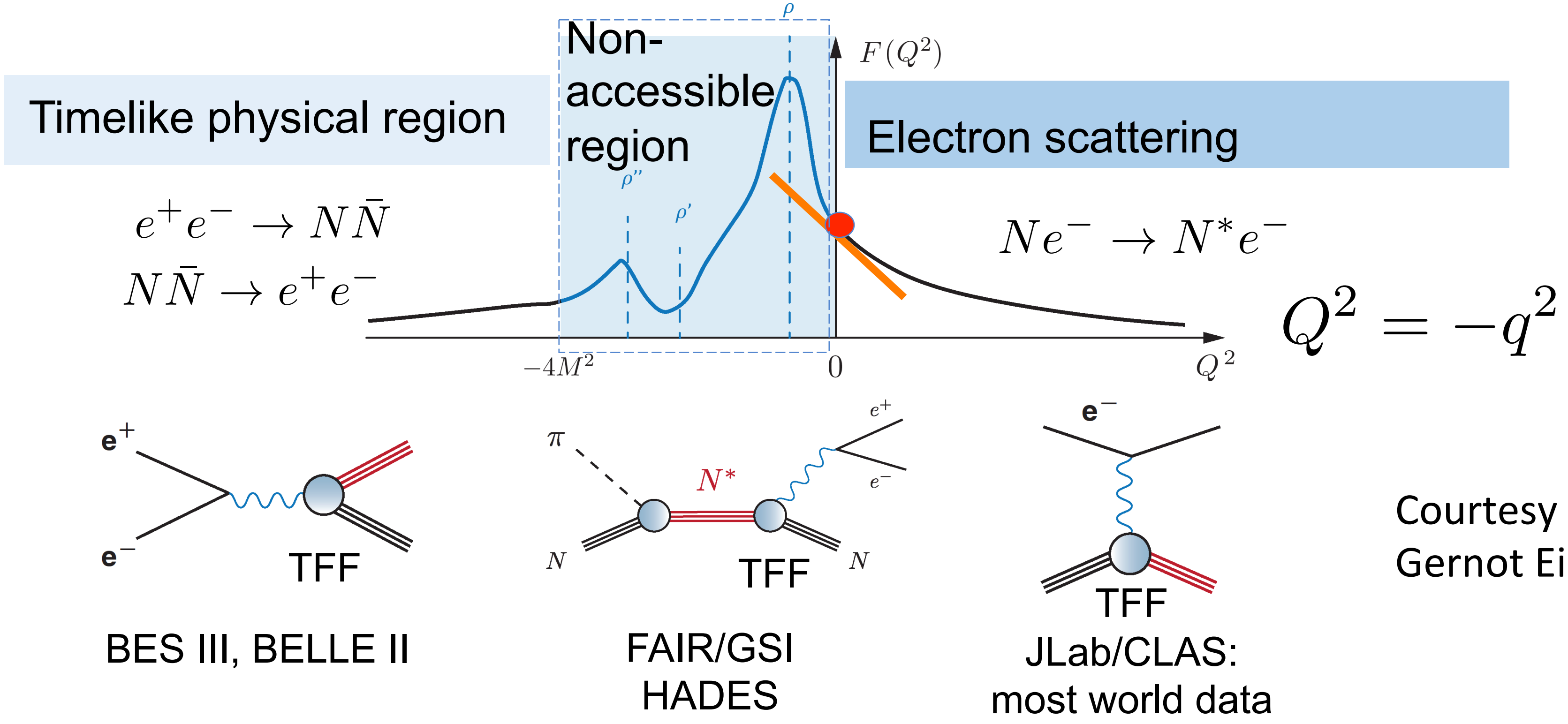

Courtesy of
Gernot Eichmann

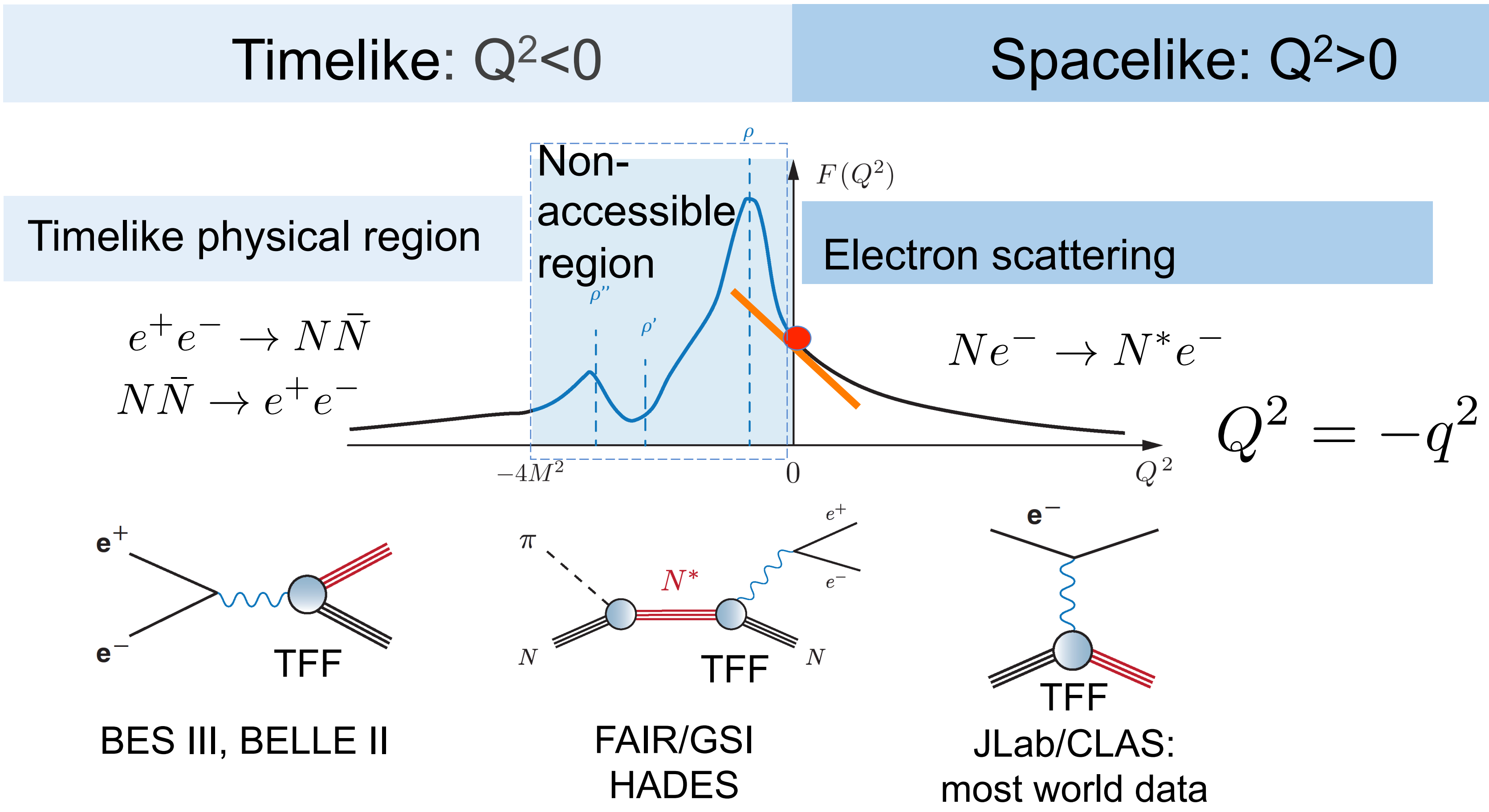

Results have to match at the photon point.
CLAS/JLab electron scattering data constrain interpretation of HADES dilepton production data.

Crossing the boundaries to explore baryon resonances

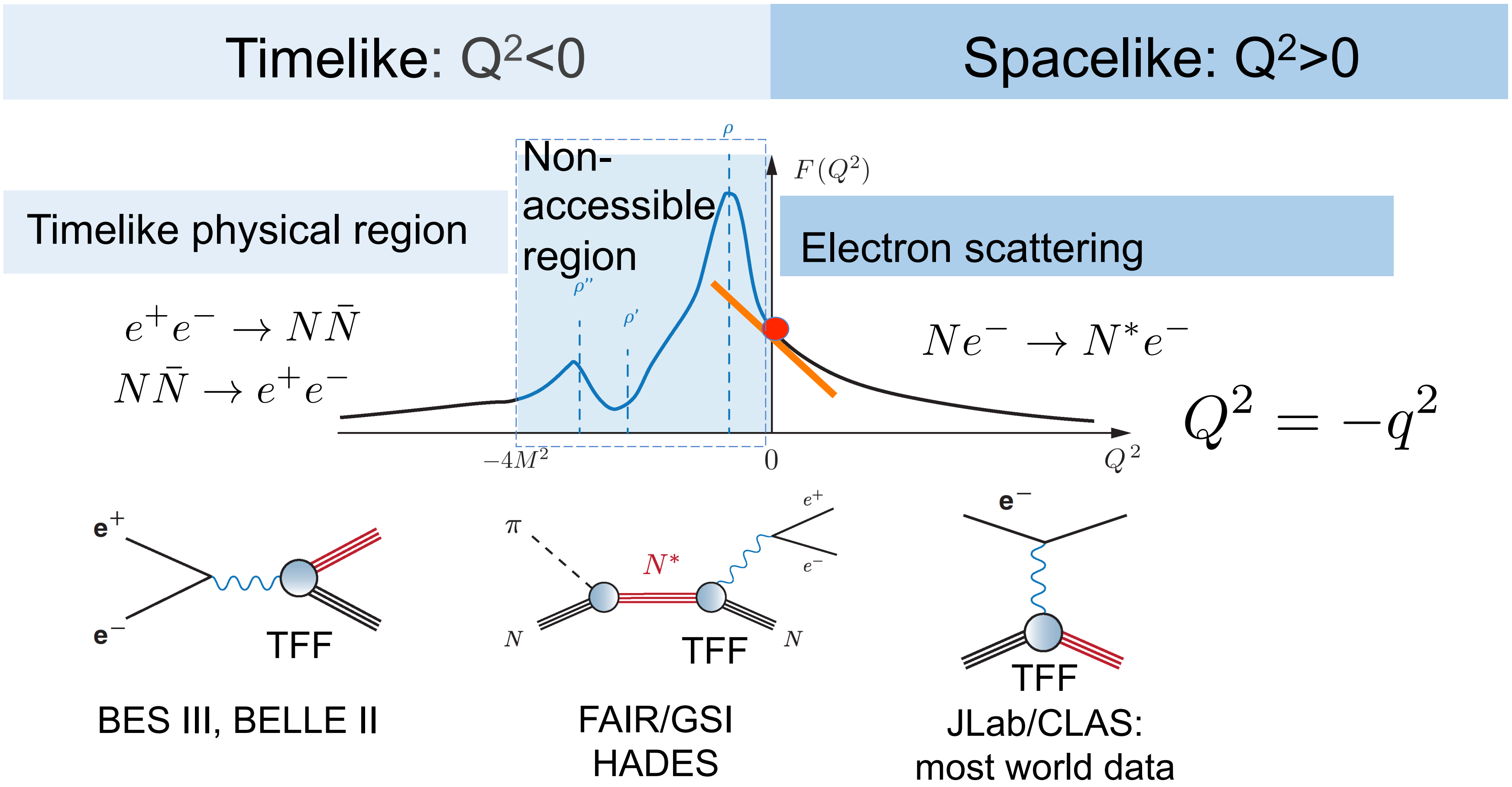

Results have to match at the photon point.
CLAS/JLab electron scattering data constrain interpretation of HADES dilepton production data.

Transition form factors

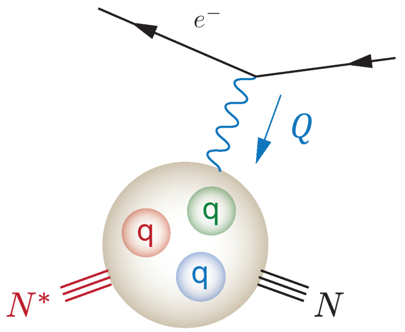

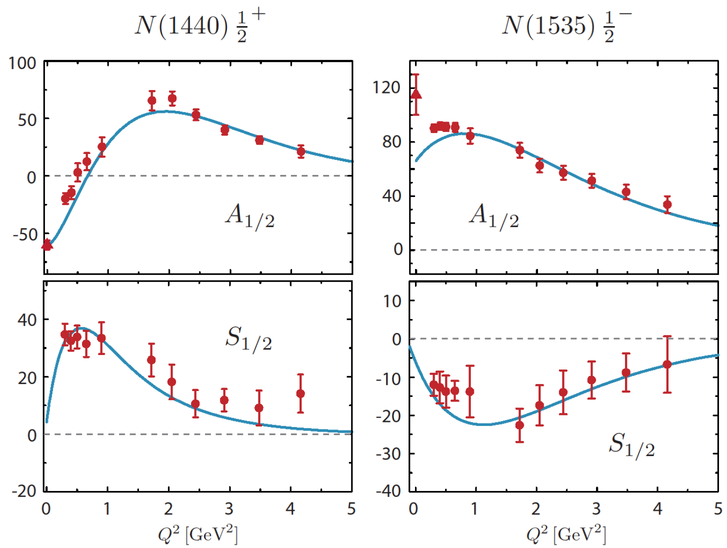

Baryon resonances
transition form factors

CLAS: Aznauryan et al., Phys. Rev. C 80 (2009)

MAID: Drechsel, Kamalov, Tiator, EPJ A 34 (2009)

See Gernot Eichmann and Gilberto Ramalho
Phys. Rev. D 98, 093007 (2018)

Spacelike form factors:

- Structure information: shape, qqq excitation vs. hybrid, ...
- Evolution of quark-photon coupling with momentum transfer

Timelike form factors:

- Particle production channels: vector mesons at small q^2
- Test of vector meson dominance
- In-medium dilepton production

This talk:
Connect Timelike and SpacelikeTransition Form Factors (TFF)
Baryon-photon coupling evolution with momentum transfer

Theoretical toolkits

Timelike baryon transition form factors not yet within reach in lattice QCD: explore alternative methods, estimate theory uncertainty!

Figs courtesy of Gernot Eichmann

- **Analyticity**

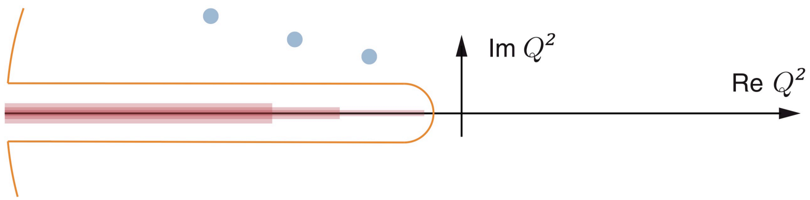

→ Dispersion theory

- **Dynamics**

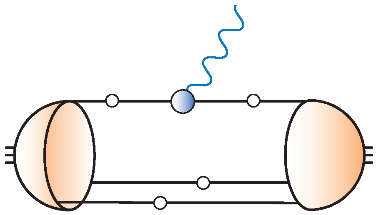

Quark-photon coupling dynamically generates VM poles!

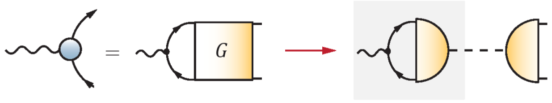

→ Dyson-Schwinger eqs.
→ Effective Lagrangian models
→ Quark models
→ Vector-meson dominance

- **Medium effects**

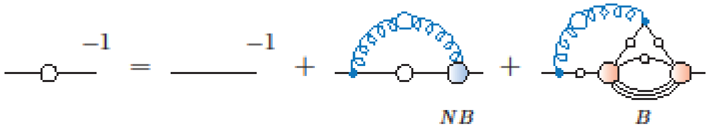

→ In-medium description of resonances!

Theoretical toolkits

Timelike baryon transition form factors not yet within reach in lattice QCD: explore alternative methods, estimate theory uncertainty!

Figs courtesy of Gernot Eichmann

- **Analyticity**

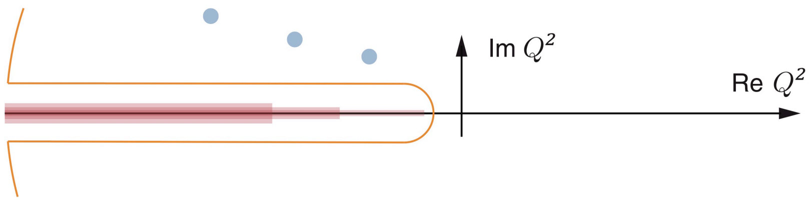

→ Dispersion theory

- **Dynamics**

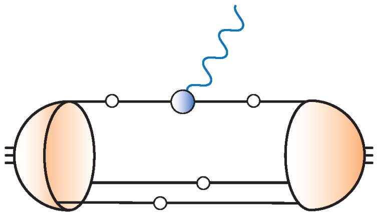

Quark-photon coupling dynamically generates VM poles!

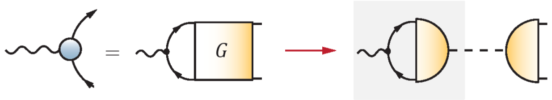

→ Dyson-Schwinger eqs.
→ Effective Lagrangian models
→ **Quark models**
→ **Vector-meson dominance**

- **Medium effects**

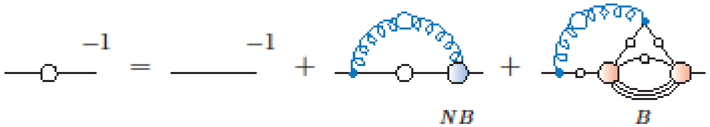

→ In-medium description of resonances!

CST© Covariant Spectator Theory

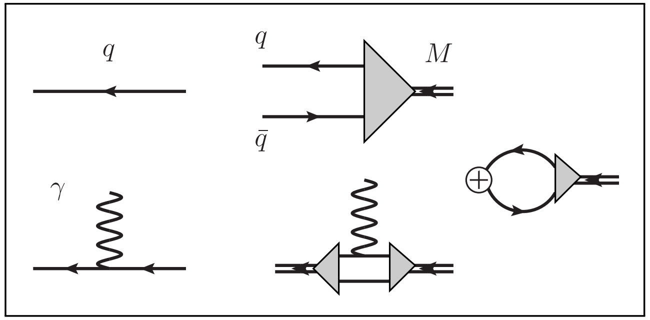

- Formulation in Minkowski space.

- Two-body CST equation effectively sums ladder and crossed-ladder exchange diagrams, due to cancelations.

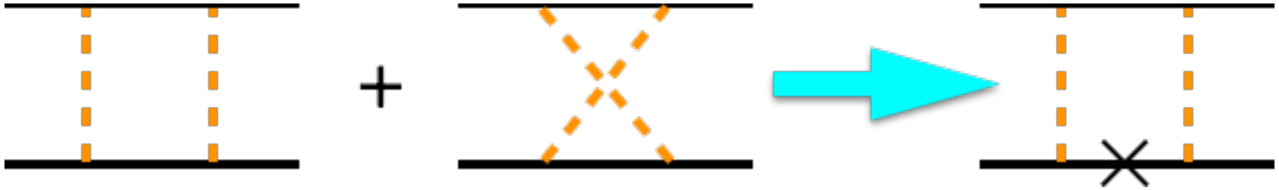

- Provides wave functions from covariant vertex with simple transformation properties under Lorentz boosts, appropriate angular momentum structures and smooth non-relativistic limit.

- Manifestly covariant, but only three-dimensional loop integrations.

$$\int_k = \int \frac{d^3\mathbf{k}}{2E_D(2\pi)^3}$$

- Allows to implement confinement and dynamical chiral symmetry breaking.

Next

1 Evidence of separation of partonic and hadronic (pion cloud) effects?
The $\Delta(1232)$ case.

2 Spacelike e.m. transition FFs:
N*(1520) and N*(1535) cases.

3 Extension to Timelike e.m. transition FFs and predictions for dilepton mass spectrum and decay widths.

4 Some predictions for Hyperons

This talk: CST phenomenological ansatz for baryon wave functions.

E.M. matrix element in Impulse Approximation

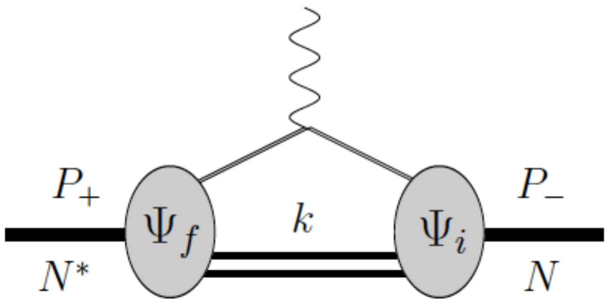

Integrate in the relative momentum of the diquark

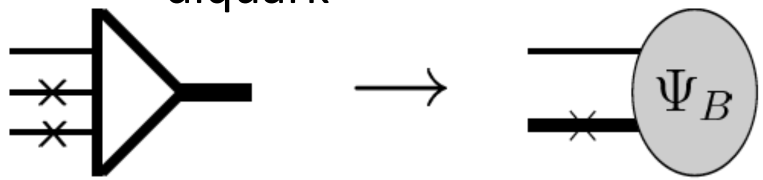

$$\int_{k_1k_2} \equiv \int \frac{d^4k_1 d^4k_2}{(2\pi)^6}\delta_+(m_1^2-k_1^2)\delta_+(m_2^2-k_2^2)$$
$$= \int \frac{d^3k_1 d^3k_2}{(2\pi)^6 4E_1E_2},$$

$$\int_{sk} = \underbrace{\int\frac{d\Omega_{\hat{\mathbf{r}}}}{4(2\pi)^3}\int_{4m_q^2}^{\infty} ds\sqrt{\frac{s-4m_q^2}{s}}}_{\int_s}\ \underbrace{\int\frac{d^3k}{(2\pi)^3 2E_s}}_{\int_k},$$

- **Baryon wavefunction** reduced to an effective quark-diquark structure due to the diquark invariant mass s integration.

- **E.M.** matrix element can be written in terms of an effective baryon composed by an off-mass-shell quark and an on-mass-shell quark pair (diquark) with an average mass.

Wave functions

Nucleon "wave function"

- A quark+ scalar-diquark component
- A quark+ **axial vector**-diquark component

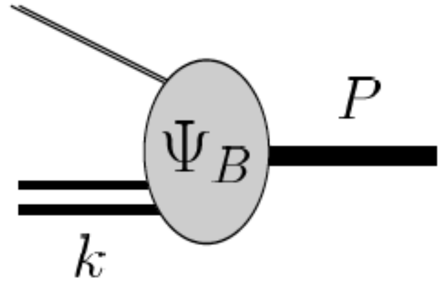

$$\Psi^S_{N\lambda_n}(P,k) = \frac{1}{\sqrt{2}}[\phi^0_I u_N(P,\lambda_n) - \phi^1_I \varepsilon^{\alpha *}_{\lambda P} U_\alpha(P,\lambda_n)]$$

$$\times \psi^S_N(P,k).$$

Phenomenological function quark-diquark momentum distribution

$$U_\alpha(P,\lambda_n) = \frac{1}{\sqrt{3}}\gamma_5\left(\gamma_\alpha - \frac{P_\alpha}{m_H}\right)u_N(P,\lambda_n),$$

Delta "wave function"

- A quark+ only **axial vector**-diquark term contributes

$$\Psi^S_\Delta(P,k) = -\psi^S_\Delta(P,k)\tilde{\phi}^1_I \varepsilon^{\beta *}_{\lambda P} w_\beta(P,\lambda_\Delta)$$

1. Evidence of separation of partonic and hadronic (pion cloud) effects?

$\Delta(1232)$

Unitarity requirements impose meson-baryon contributions to the electromagnetic excitation and decay of baryons

Bare quark and pion cloud components

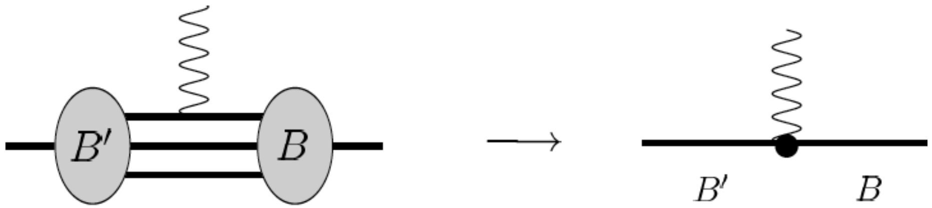

For low Q² : add coupling with pion in flight.

Bare quark component

Pion cloud

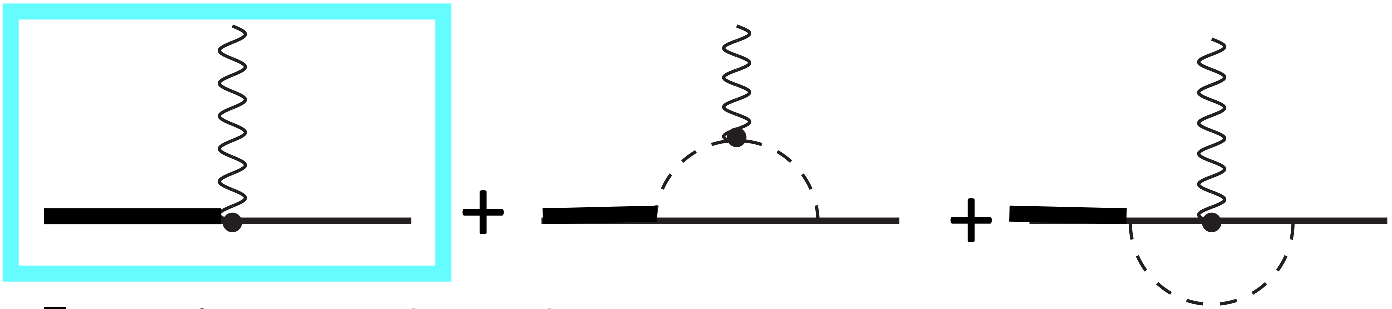

$q\bar{q}$ pairs from a single quark included in dressing

Pion created by the overall baryon, not from a single quark

Pion cloud component supressed for high Q² $\frac{1}{Q^8}$

Model independent feature

$$\gamma N \rightarrow \Delta \qquad G_M^* = G_M^B + G_M^\pi$$

Separation seems to be supported by experiment.
Missing strength of G_M at the origin is an universal feature, even in dynamical quark calculations.

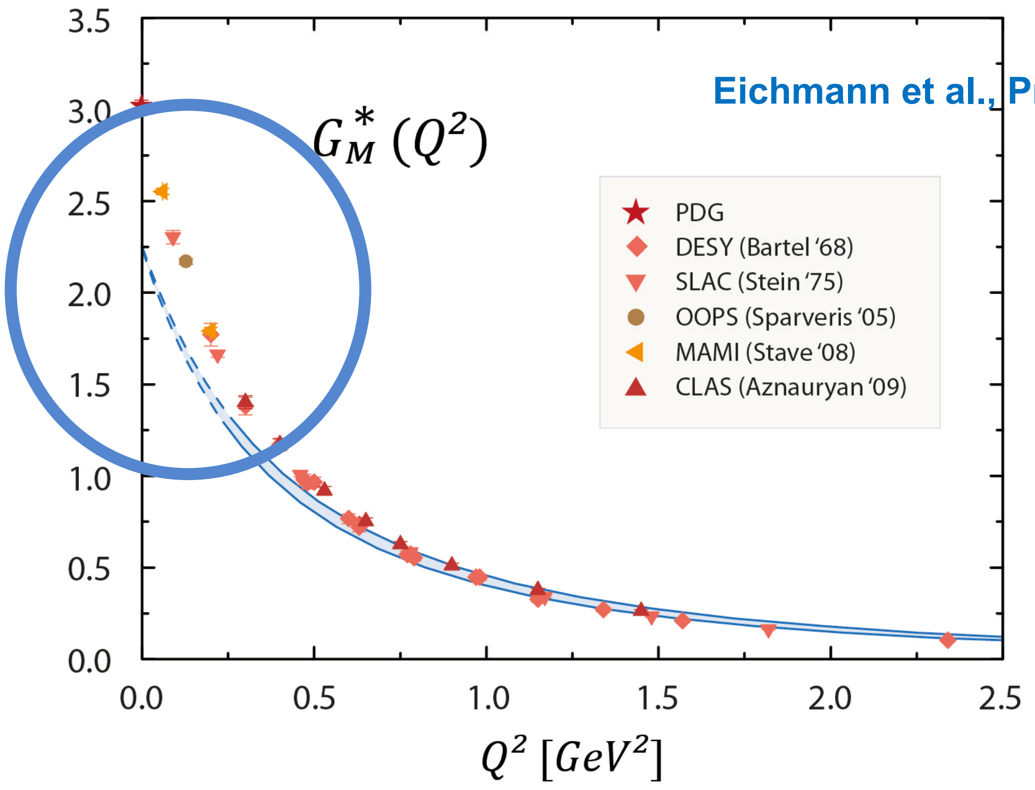

Eichmann et al., Prog. Part. Nucl. Phys. 91 (2016)c

Effect of vicinity of the mass pole of the Delta to the pion-nucleon threshold.

Model independent feature

$$\gamma N \rightarrow \Delta \qquad G_M^* = G_M^B + G_M^\pi$$

Separation seems to be supported by experiment.
Missing strength of G_M at the origin is an universal feature.

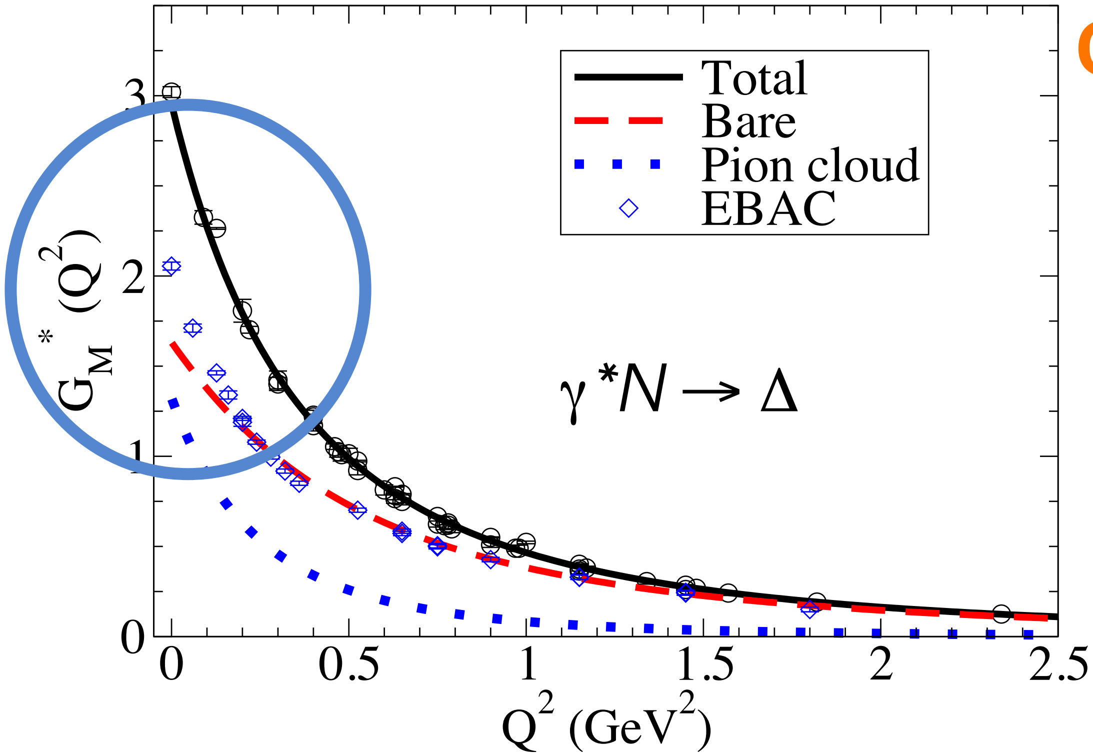

CST© 2009

Bare quark core:

- dominates large Q^2 region.
- agrees with EBAC analysis.

E.M. Current

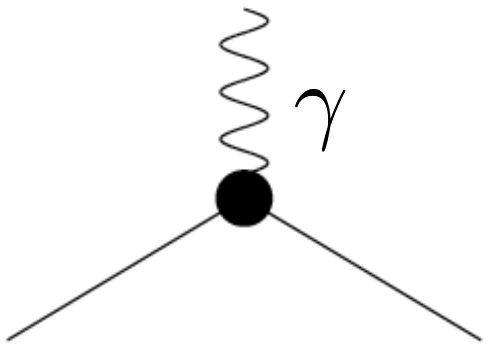

quark-antiquark

⊕ gluon dressing

Quark form factors f adjusted to quark charges and anomalous magnetic moments, such that experimental magnetic moments of the nucleons are reproduced.

Constituent quarks (quark form factors)

$$j_I^\mu = \left[\frac{1}{6}f_{1+} + \frac{1}{2}f_{1-}\tau_3\right]\gamma^\mu + \left[\frac{1}{6}f_{2+} + \frac{1}{2}f_{2-}\tau_3\right]\frac{i\sigma^{\mu\nu}q_\nu}{2M_N}$$

E.M. Current

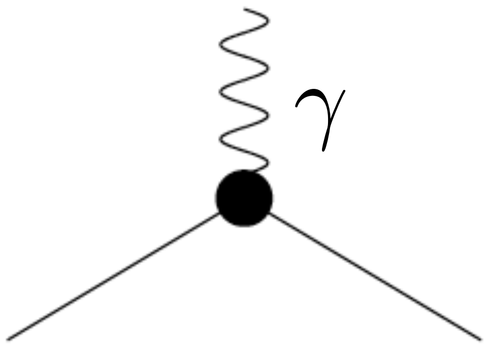

quark-antiquark
$\oplus$ gluon dressing

Processes where pions are created and absorbed by the same quark are included in the constituent quark internal structure, and thus included in the quark current.

Constituent quarks (quark form factors)

$$j_I^\mu = \left[\frac{1}{6} f_{1+} + \frac{1}{2} f_{1-} \tau_3\right] \gamma^\mu + \left[\frac{1}{6} f_{2+} + \frac{1}{2} f_{2-} \tau_3\right] \frac{i\sigma^{\mu\nu} q_\nu}{2M_N}$$

E.M. Current

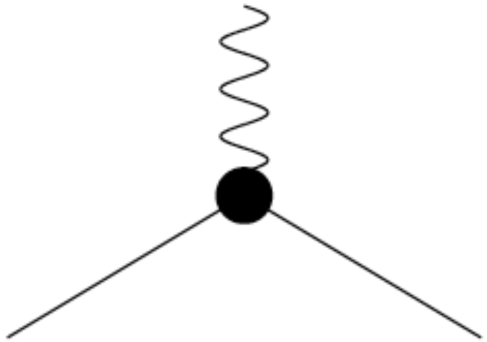

quark-antiquark

⊕ gluon dressing

Meson spectrum ties with the behavior of the quark photon coupling.

To parametrize the current use **VMD**, a truncation to the ρ pole of the full meson spectrum contribution to the quark-photon coupling.

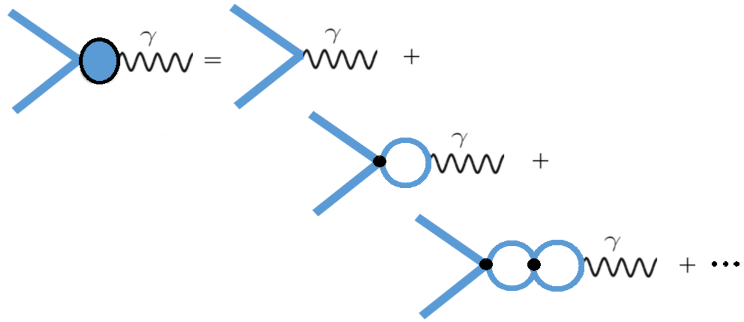

Constituent quarks (quark form factors)

$$j_I^\mu = \left[\frac{1}{6} f_{1+} + \frac{1}{2} f_{1-} \tau_3\right] \gamma^\mu + \left[\frac{1}{6} f_{2+} + \frac{1}{2} f_{2-} \tau_3\right] \frac{i\sigma^{\mu\nu} q_\nu}{2M_N}$$

$$\Gamma_\mu(p,Q) = \gamma_\mu + \int \frac{d^4q}{(2\pi)^4} K(p,q,Q) S(q+\eta Q) \Gamma_\mu(q,Q) S(q-\eta Q)$$

Vector meson dominance **2** poles

$$f(Q^2) = e + gB(Q^2)e + gB(Q^2)gB(Q^2)e + \cdots = e + \frac{gB(Q^2)e}{1-gB(Q^2)}$$

if $gB(Q^2) = \frac{\lambda^2}{\Lambda^2+Q^2}$, then $f(Q^2) = e + \frac{\lambda^2 e}{\Lambda^2-\lambda^2+Q^2}$

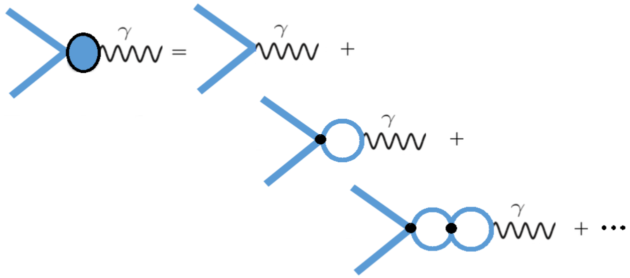

$$\Gamma_\mu(p,Q) = \gamma_\mu + \int \frac{d^4q}{(2\pi)^4} K(p,q,Q) S(q+\eta Q)\Gamma_\mu(q,Q)S(q-\eta Q)$$

$$f_{1+} = \lambda + \frac{1-\lambda}{1+Q_0^2/m_v^2} + \frac{c_\pm Q_0^2/M_h^2}{\left(1+Q_0^2/M_h^2\right)^2}$$

$$f_{2\pm} = \kappa_\pm\left(\frac{d_\pm}{1+Q_0^2/m_v^2} + \frac{(1-d_\pm)}{1+Q_0^2/M_h^2}\right)$$

Low-energy behavior encodes high-energy behavior: Scale enters in the problem! DIS used to fixed λ

4 parameters

VMD as link to LQCD

- VMD enables link to LQCD:

in the current the vector meson mass is taken as a function of the running pion mass.

- Pion cloud contribution negligible for **large pion masses**,

and **bare** quark model could be calibrated to the **lattice data.**

- After that, in the limit of the physical pion mass value,

the **experimental data** is well described in the large Q^2 region.

Connection to Lattice QCD

To control model dependence:

CST model and LQCD data are made **compatible.**

G. Ramalho and M. T. Peña, Phys. Rev. D 80, 013008 (2009)

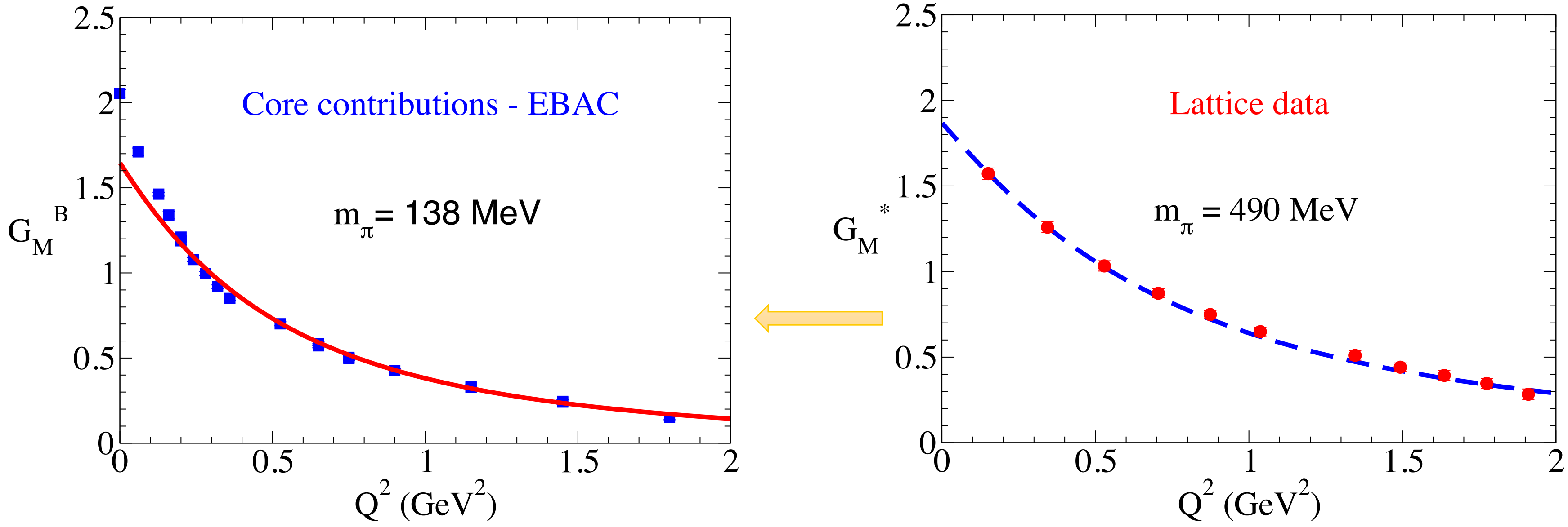

Model (no pion cloud) valid for lattice pion mass regime.
No refit of wave function scale parameters for the physical pion mass limit.

E.M. Current and TFF at the photon point

$$\gamma N \rightarrow \Delta$$

$$\Gamma^{\beta\mu}(P,q) = \left[G_1 q^\beta \gamma^\mu + G_2 q^\beta P^\mu + G_3 q^\beta q^\mu - G_4 g^{\beta\mu}\right]\gamma_5$$

- Only 3 G_i are independent:
  E.M. Current has to be conserved $q^\mu \Gamma_{\beta\mu} = 0$

  → G_M, G_E, G_C Scadron Jones popular choice.

- Only finite G_i are physically acceptable.

Orthogonality between initial and final states necessarily follows from both requirements, giving an important constraint to G_c at $Q^2=0$.

2. Spacelike e.m. transition FFs

N*(1520), N*(1535)

$N \to N^*(1520)$ **Helicity amplitudes**

$J^P=3/2^-$ I=1/2
60% decay to πN
30% decay to $\pi\Delta$

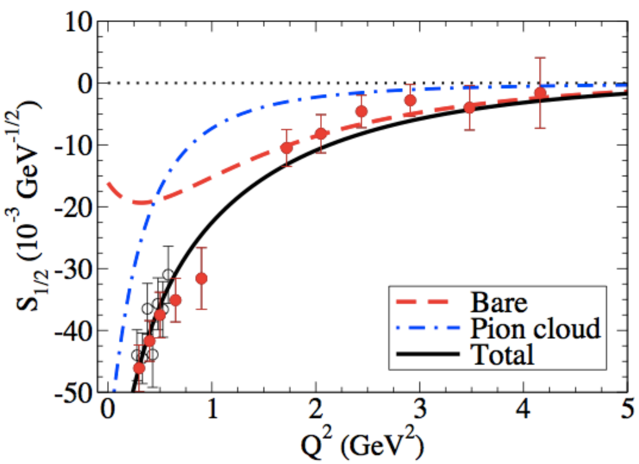

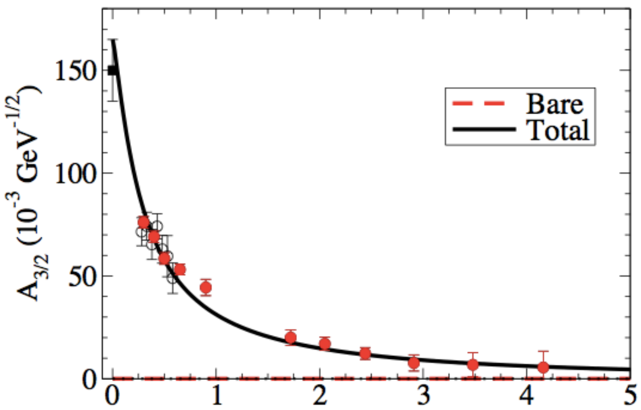

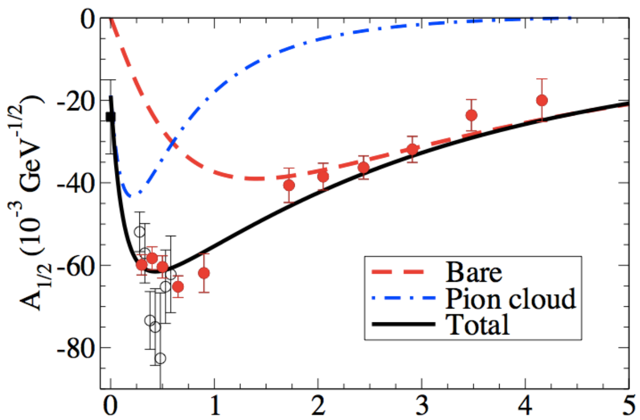

- Bare quark model gives good description of high Q^2 region.

- Use CST quark model to infer meson cloud from the data.

G. Ramalho, M. T. P. , PHYSICAL REVIEW D 85 094016 (2014)

$N \rightarrow N^*(1520)$ Helicity amplitudes

$J^P=3/2^-$ I=1/2
60% decay to πN
30% decay to $\pi\Delta$

- Bare quark model gives good description of high Q^2 region

- No bare quark contribution to $A_{3/2}$.

G. Ramalho, M. T. P. , PHYSICAL REVIEW D 85 094016 (2014)

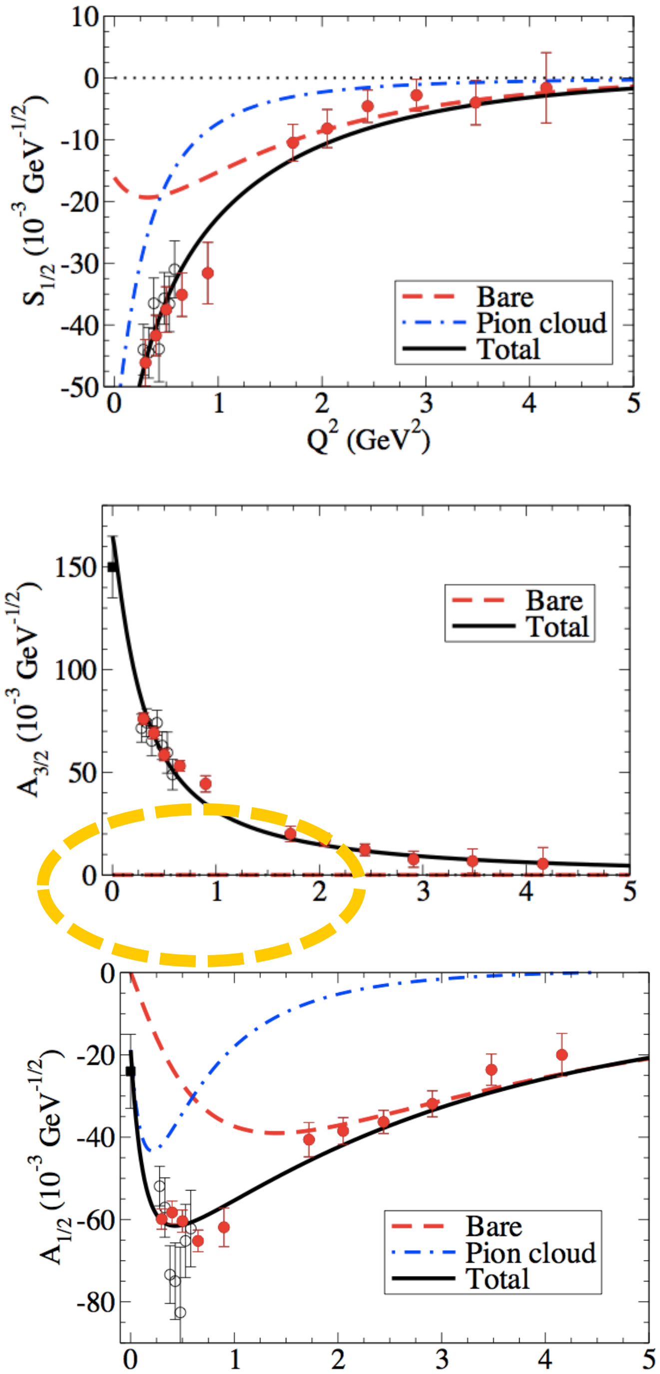

$N \rightarrow N^*(1520)$ TFFs

Transition Form Factors, Scadron and Jones convention

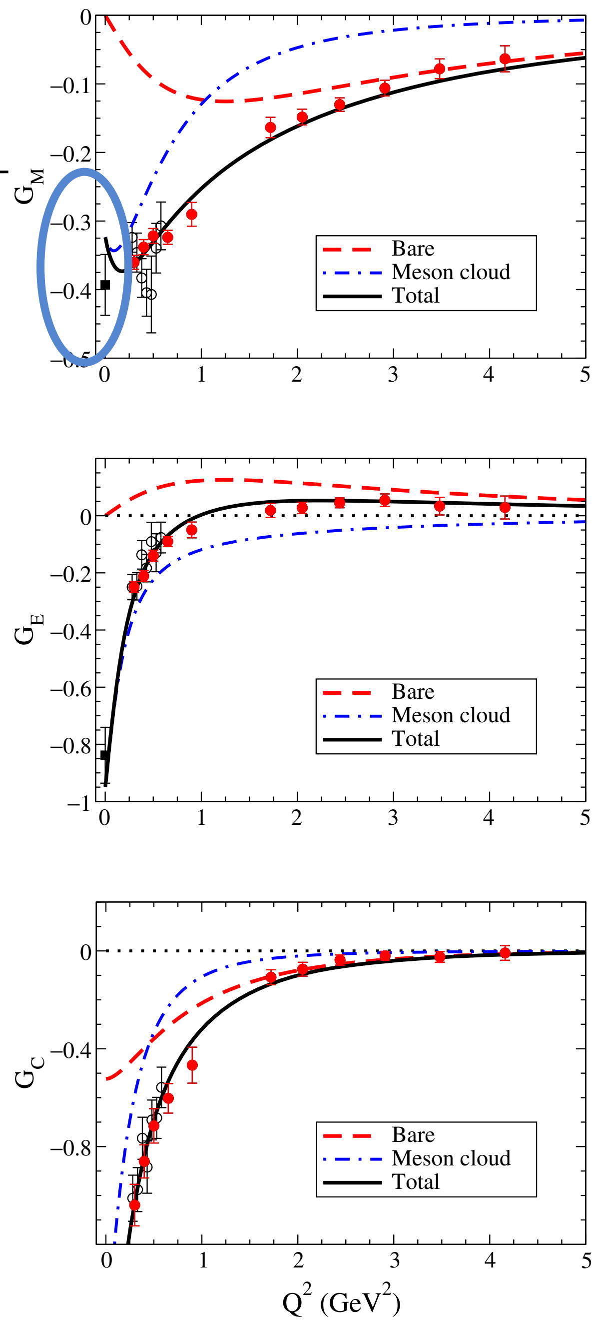

- Underestimation of G_M close to the photon point due to overall fit.

- Important role of meson cloud;

dominated by the pion due to the πN and $\pi\Delta$ channels branching ratios.

(as in Aznauryan and Burkert, PRC 85 055202 2012)

G. Ramalho, M. T. P. ,PHYSICAL REVIEW D 95 014003 (2017)

$N \to N^*(1520)$

PDG data at the photon point:

	$A_{1/2}$	$A_{3/2}$	$\|A\|^2$
p	-0.025 ± 0.005	0.140 ± 0.005	20.2 ± 1.4
n	-0.050 ± 0.005	-0.120 ± 0.005	15.7 ± 1.3

$$A^V_{3/2} \approx 0.13 \; ; A^S_{3/2} \approx 0.01 \, (GeV^{-1/2})$$

Dominance of iso-vector channel concurs to our model of the meson cloud: pion only

$N \rightarrow N^*(1535)$ **TFFs**

$J^P = 1/2^-$ I=3/2
~50% decay to πN
~50% decay to ηN

$$J^\mu = \bar{u}_R \left[F_1^* \left(\gamma^\mu - \frac{\not{q} q^\mu}{q^2} \right) + F_2^* \frac{i\sigma^{\mu\nu} q_\nu}{M_N + M_R} \right] \gamma_5 u_N$$

- Use CST quark model to infer meson cloud from the data. Again good agreement of bare quark core with EBAC analysis

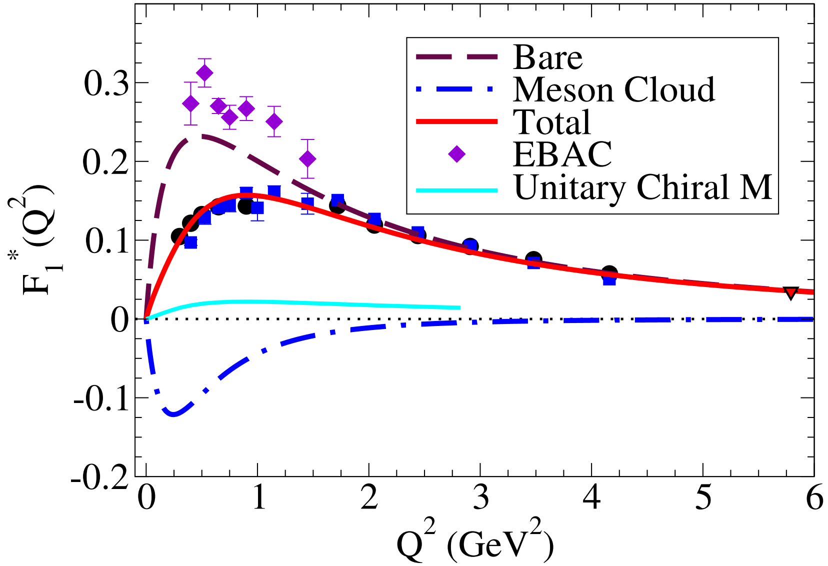

- Bare quark effects dominate F_1^* for large Q^2

- Meson cloud effects dominate F_2^* with meson cloud extending to high Q^2 region.

(effect from the η N channel?).

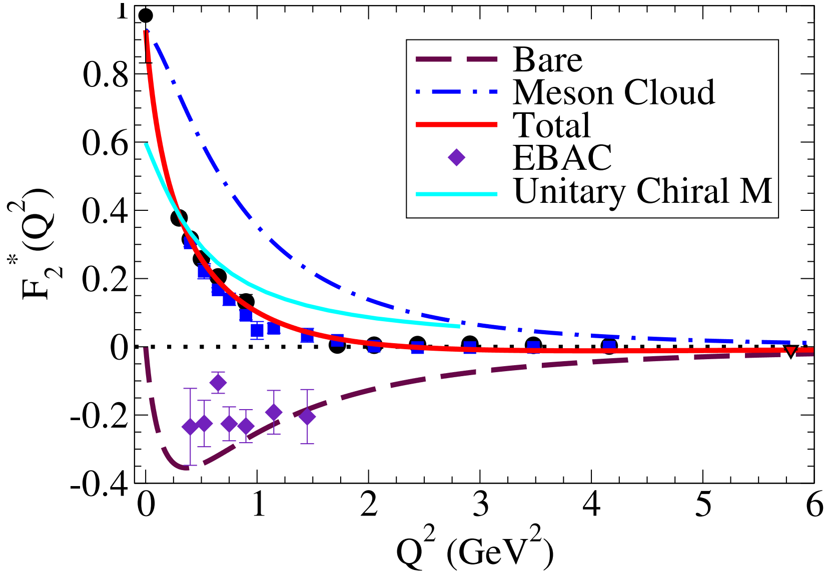

$N \rightarrow N^*(1535)$

Iso-vector + iso-scalar channels included into our model of the meson cloud: pion and eta cloud.

$$F_1^{\mathrm{MC}} = Q^2 \tilde{C}(Q^2)\tau_3 \qquad\qquad F_2^{\mathrm{MC}} = A(Q^2) + B(Q^2)\tau_3$$

PDG data at the photon point:

$$A^V_{1/2}(0) = 0.090 \pm 0.013 \ \mathrm{GeV}^{-1/2}$$

$$A^S_{1/2}(0) = 0.015 \pm 0.013 \ \mathrm{GeV}^{-1/2}$$

Isovector dominance to some extent

3. Extension to Timelike

Δ (1232),

N*(1520), N*(1535)

Extension to Timelike

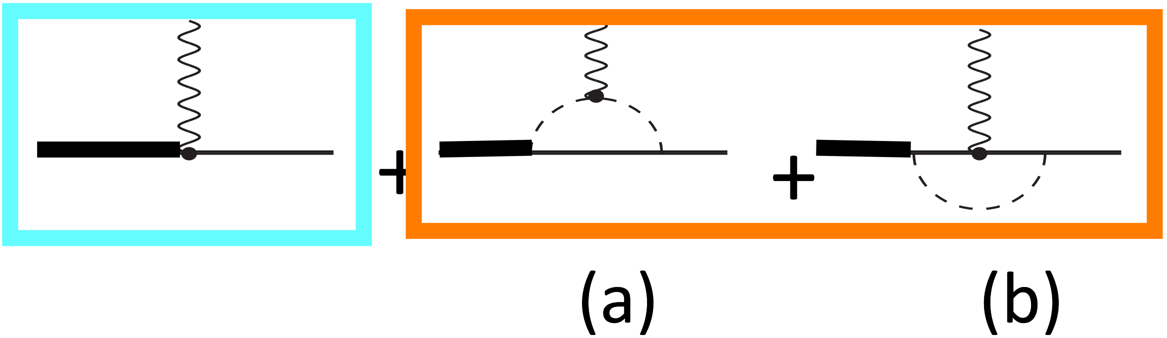

The residue of the pion from factor $F_\pi(q^2)$ at the timelike ρ pole is proportional to the $\rho \to \pi\pi$ decay

Extension to Timelike

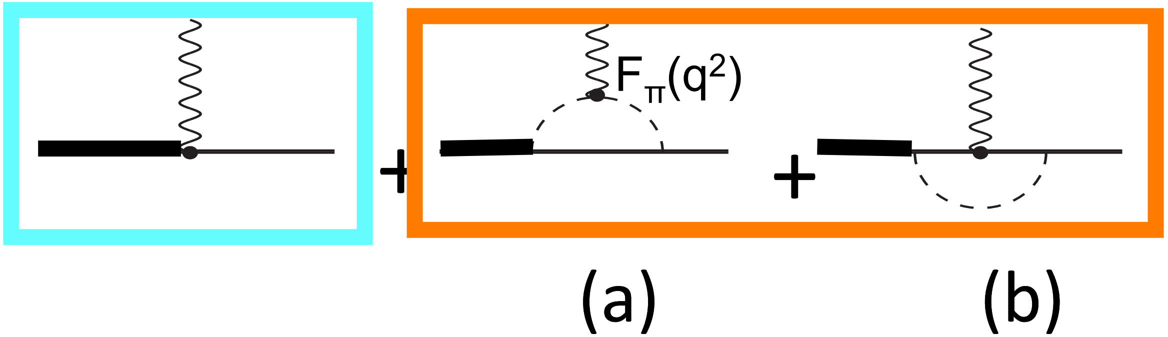

The residue of the pion from factor $F_\pi(q^2)$ at the timelike ρ pole is proportional to the $\rho \longrightarrow \pi\pi$ decay

Diagram (a) related with pion electromagnetic form factor $F_\pi(q^2)$

Extension to Timelike

Parametrization of pion Form Factor

$$F_\pi(q^2) = \frac{\alpha}{\alpha - q^2 - \frac{1}{\pi}\beta q^2 \log \frac{q^2}{m_\pi^2} + i\beta q^2}$$

$\alpha = 0.696$ GeV^2

$\beta = 0.178$

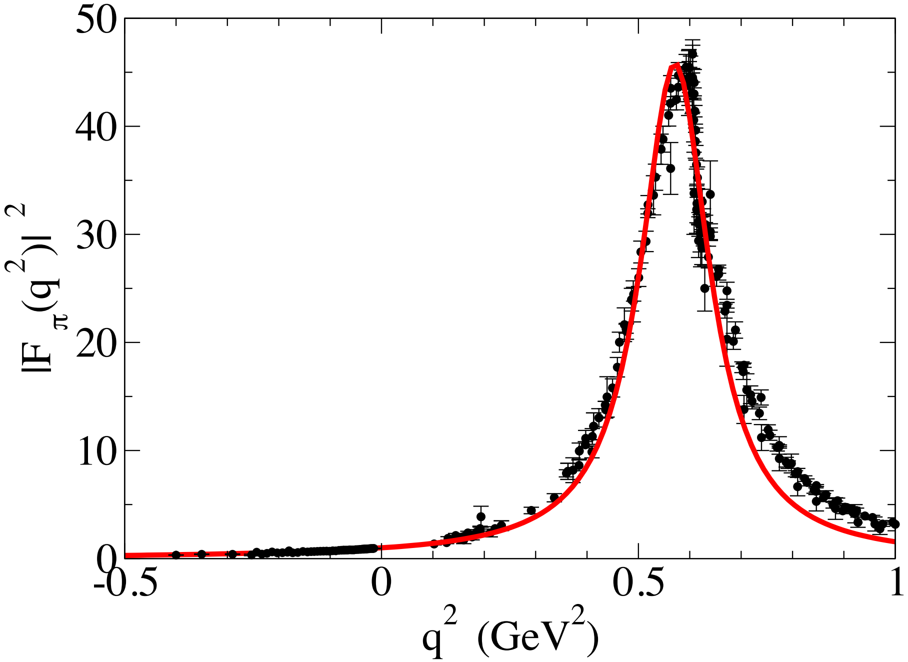

Extension to Timelike

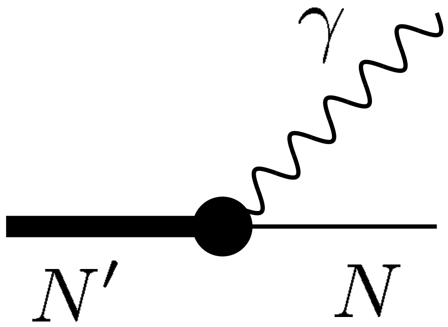

R rest frame

$$P_R = (W, 0, 0, 0); \quad P_N = (E_N, 0, 0, -|\mathbf{q}|); \quad q = (\omega, 0, 0, |\mathbf{q}|)$$

Timelike $q^2 > 0$

$$\omega = \frac{W^2 - M^2 + q^2}{2W}$$

$$|\mathbf{q}|^2 = \frac{[(W+M) - q^2][(W-M)^2 - q^2]}{4W^2}$$

$$E_N = \frac{W^2 + M^2 - q^2}{2W}$$

Spacelike $-q^2 = Q^2 > 0$

$$\omega = \frac{W^2 - M^2 - Q^2}{2W}$$

$$|\mathbf{q}|^2 = \frac{[(W+M) + Q^2][(W-M)^2 + Q^2]}{4W^2}$$

$$E_N = \frac{W^2 + M^2 + Q^2}{2W}$$

TL: $q^2 \leq (W-M)^2$

$W \geq M$

Transition form factors in the timelike region are restricted to a given kinematic region that depends on the varying resonance mass W.

Extension to Timelike

$$\gamma N \rightarrow \Delta$$

- Extension to higher W shows effect of the rho mass pole
- In that pole region small bare quark contribution (thin lines)

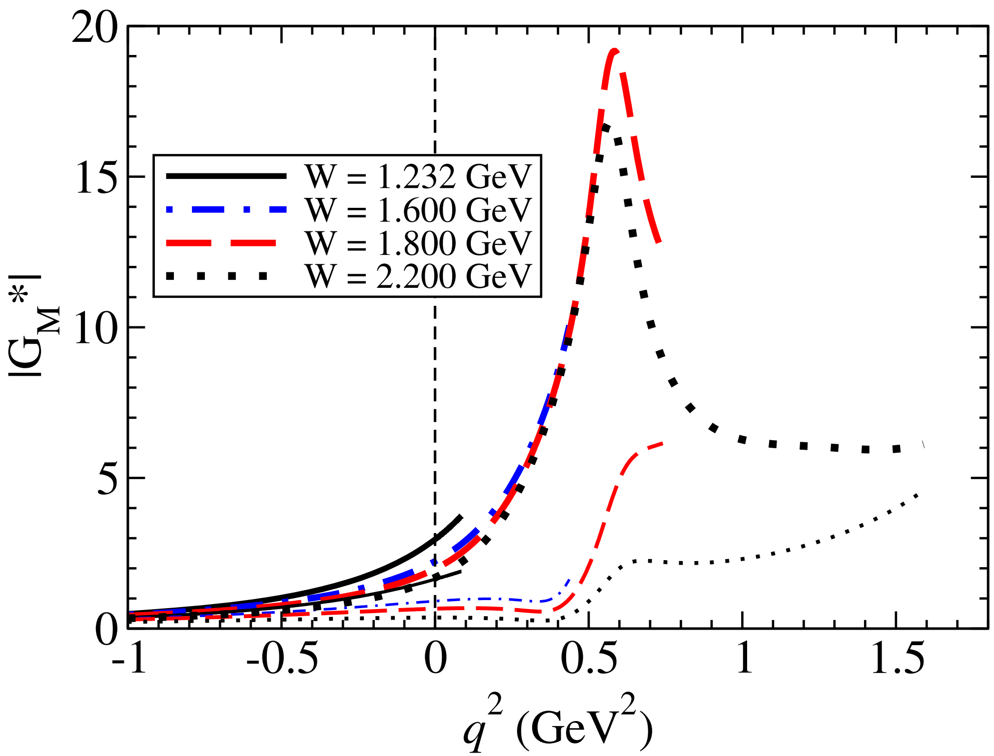

Crossing the boundaries

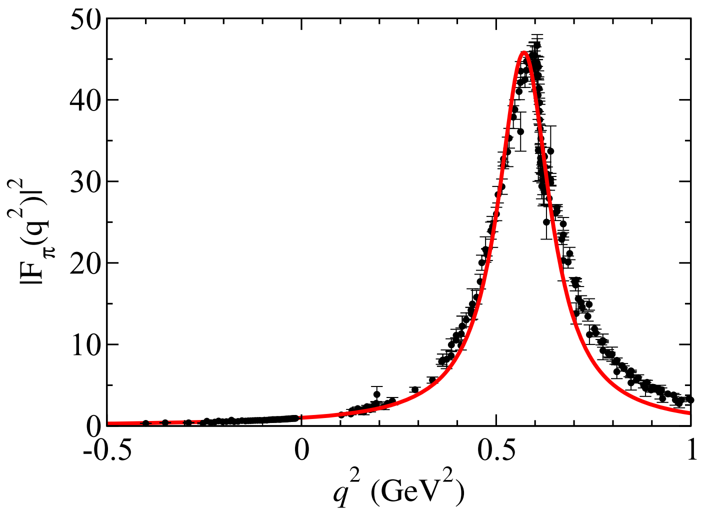

$\gamma N \rightarrow \Delta$

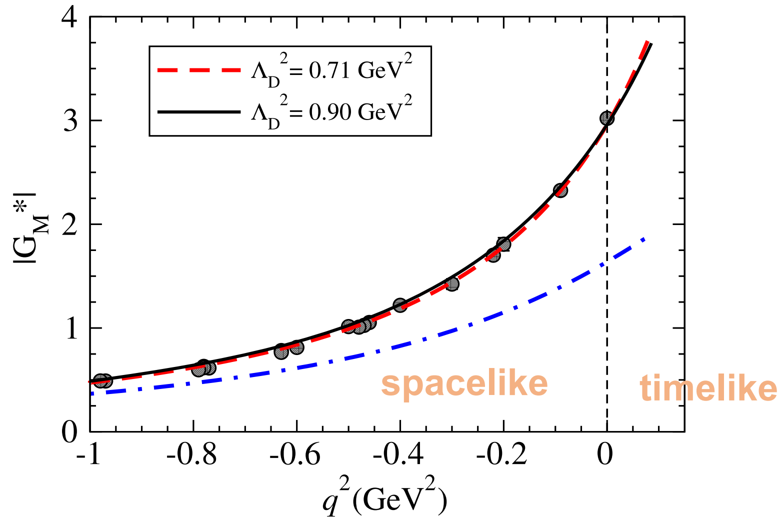

Red line : full model
Blue line: Quark core

- Good description of the magnetic dipole physical data ($W = M_\Delta$)

Crossing the boundaries

Δ(1232) Dalitz decay

$$\Gamma_{\gamma^* N}(q;W) = \frac{\alpha}{16}\frac{(W+M)^2}{M^2W^3}\sqrt{y_+y_-}y_-|G_T(q^2,W)|^2$$

$$|G_T(q^2;M_\Delta)|^2 = |G_M^*(q^2;W)|^2 + 3|G_E^*(q^2;W)|^2 + \frac{q^2}{2W^2}|G_C^*(q^2;W)|^2$$

$$y_\pm = (W \pm M)^2 - q^2$$

$$\Gamma_{\gamma N}(W) \equiv \Gamma_{\gamma^* N}(0;W)$$

$$\Gamma_{e^+e^-N}(W) = \frac{2\alpha}{3\pi}\int_{2m_e}^{W-M} \Gamma_{\gamma^* N}(q;W)\frac{dq}{q}$$

Crossing the boundaries

Δ(1232) Dalitz decay

Ramalho, Pena, Weil, Van Hees, Mosel, Phys.Rev. C93 (2016)

$$\gamma N \rightarrow \Delta$$

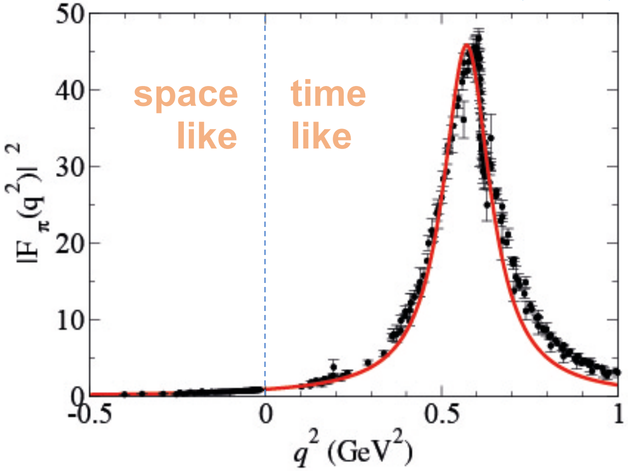

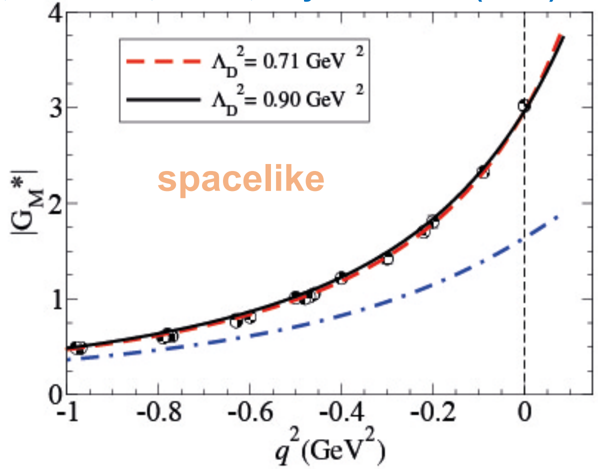

HADES Collaboration, Phys.Rev. C95 (2017)

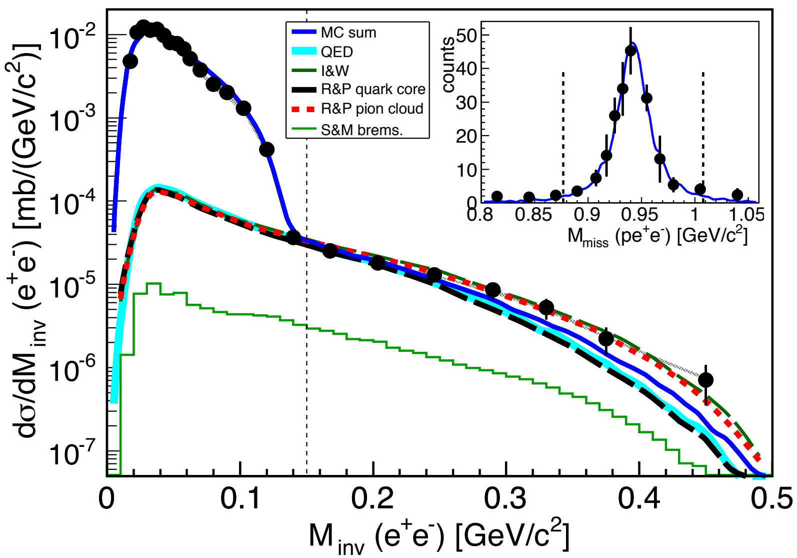

Δ Dalitz decay branching ratio 4.19 x 10^{-5}

Crossing the boundaries

Δ(1232) Dalitz decay

$$\gamma N \rightarrow \Delta$$

Ramalho, Pena, Weil, Van Hees, Mosel, Phys.Rev. C93 (2016)

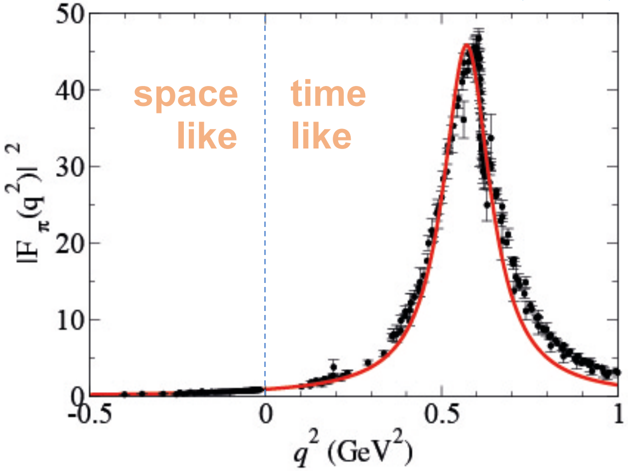

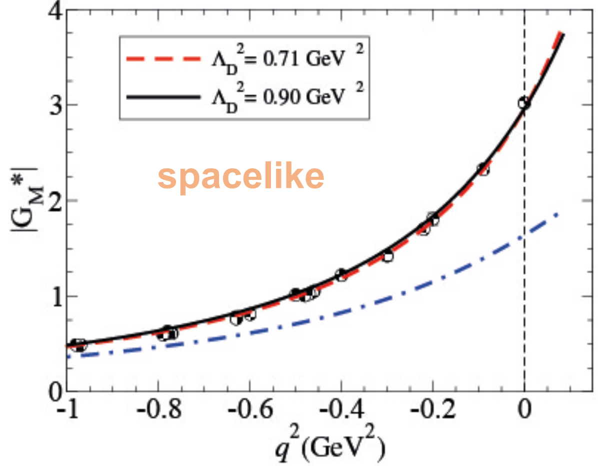

HADES Collaboration, Phys.Rev. C95 (2017)

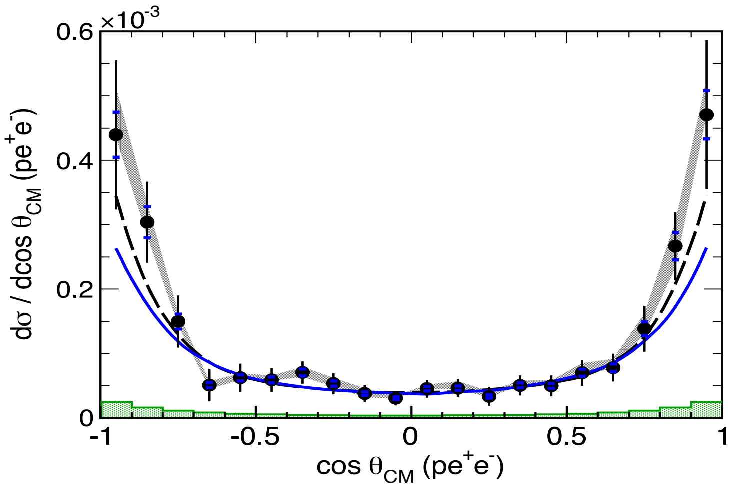

Angular distribution for pe$^+$e$^-$

Crossing the boundaries

N*(1520)

$$\Gamma_{\gamma^* N}(q,W) = \frac{3\alpha}{32}\frac{(W-M)^2}{M^2W^3}\sqrt{y_+y_-}y_+|G_T(q^2,W)|^2$$

$$y_\pm = (W \pm M)^2 - q^2$$

$$|G_T(q^2,W)|^2 = 3|G_M(q^2,W)|^2 + |G_E(q^2,W)|^2 + \frac{q^2}{2W^2}|G_C(q^2,W)|^2.$$

Amplifies q^2 dependence

$$\Gamma'_{e^+e^-N}(q,W) \equiv \frac{d\Gamma}{dq}(q,W) = \frac{2\alpha}{3\pi q^3}(2\mu^2+q^2)\sqrt{1-\frac{4\mu^2}{q^2}}\Gamma_{\gamma^* N}(q,W)$$

G. Ramalho, M. T. P. , PHYSICAL REVIEW D 95 0104003 (2017)

Crossing the boundaries

N*(1520)

True prediction

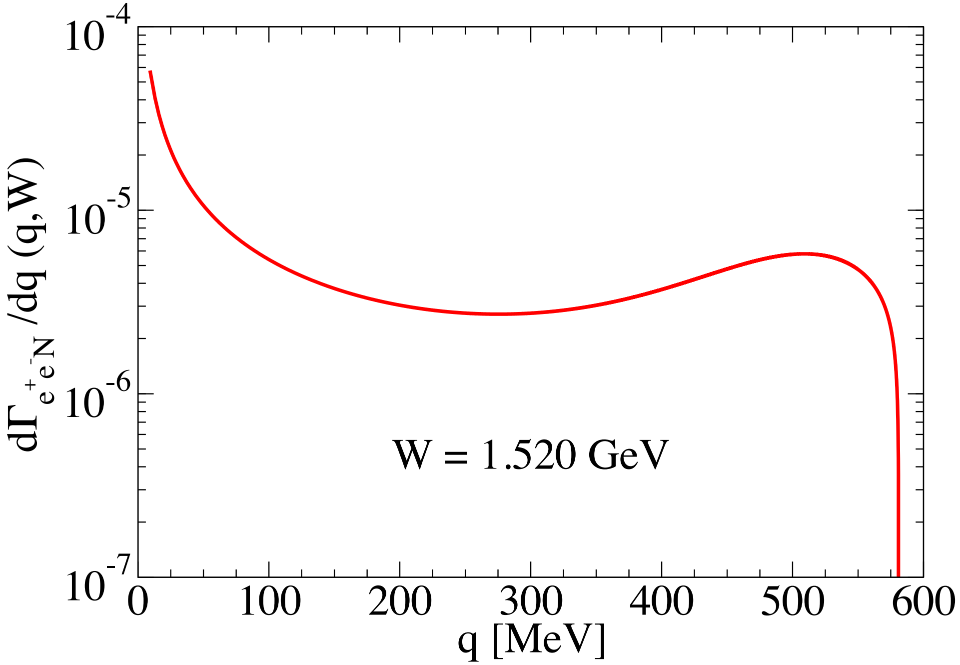

G. Ramalho, M. T. P. , PHYSICAL REVIEW D 95 0104003 (2017)

Crossing the boundaries

N*(1520)

True prediction

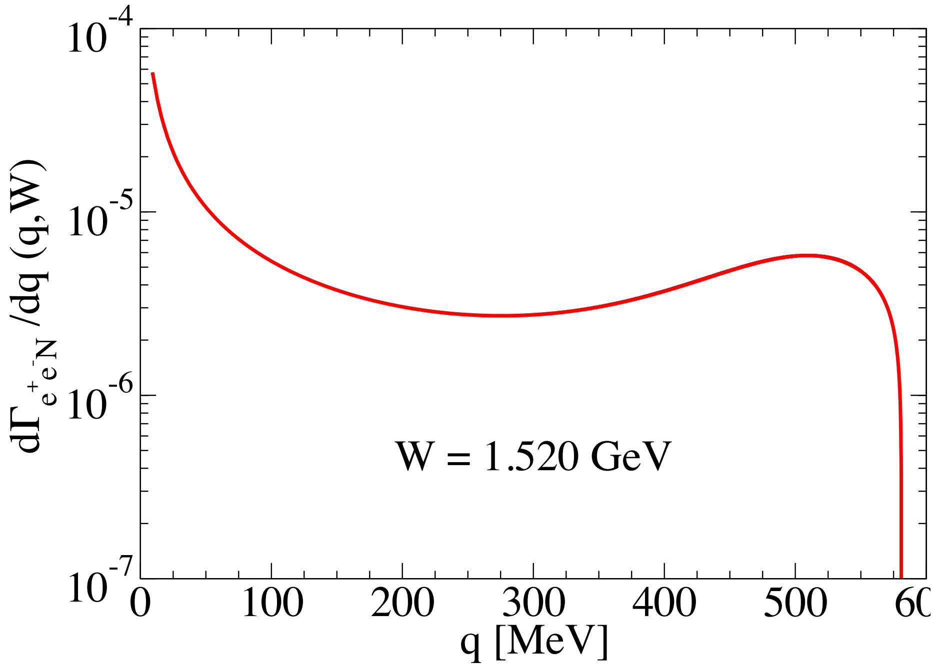

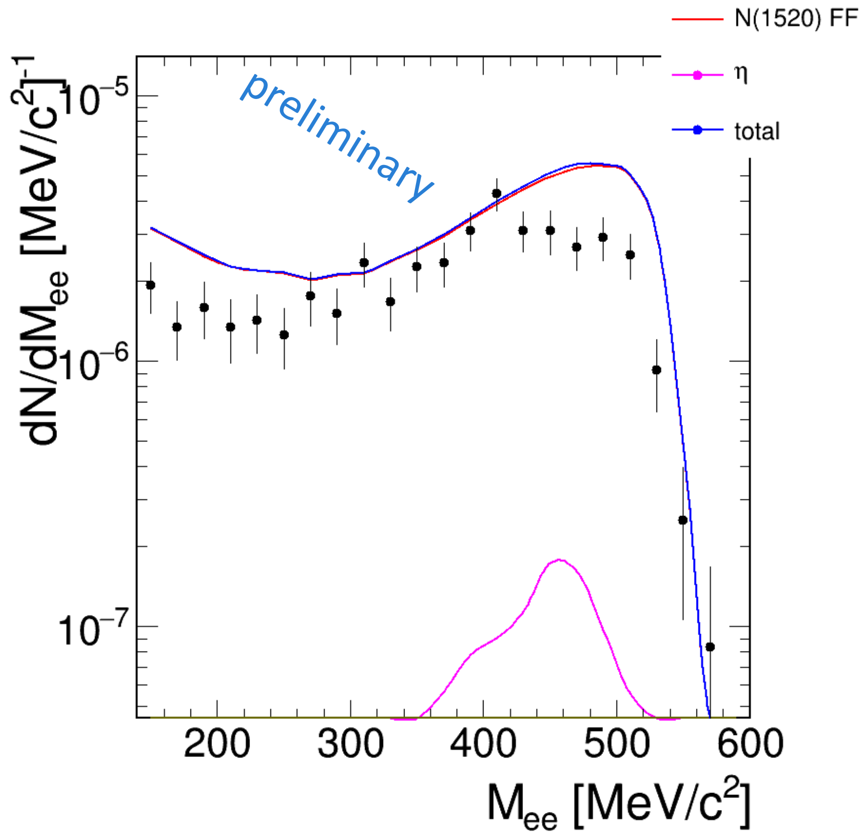

HADES Collaboration
2018

Crossing the boundaries

N*(1520)

2017 results

Proton

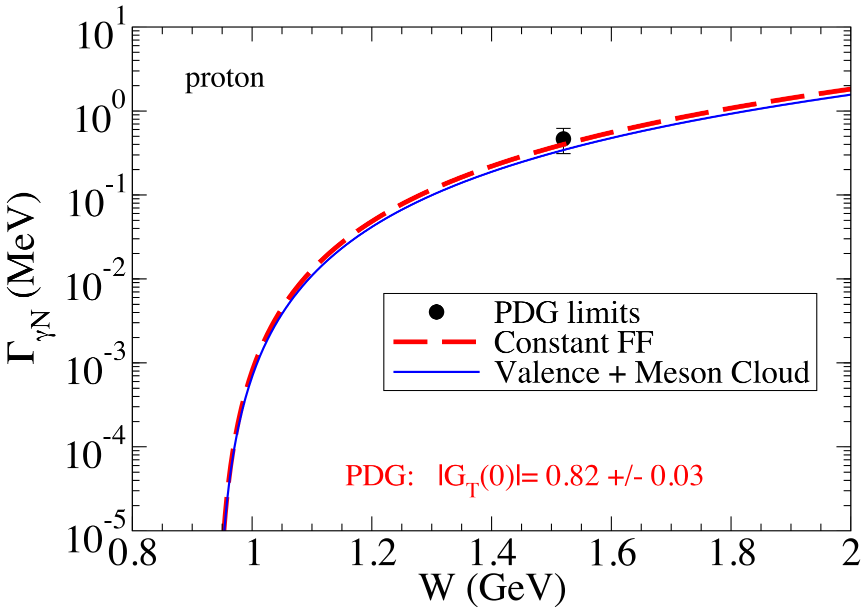

Neutron

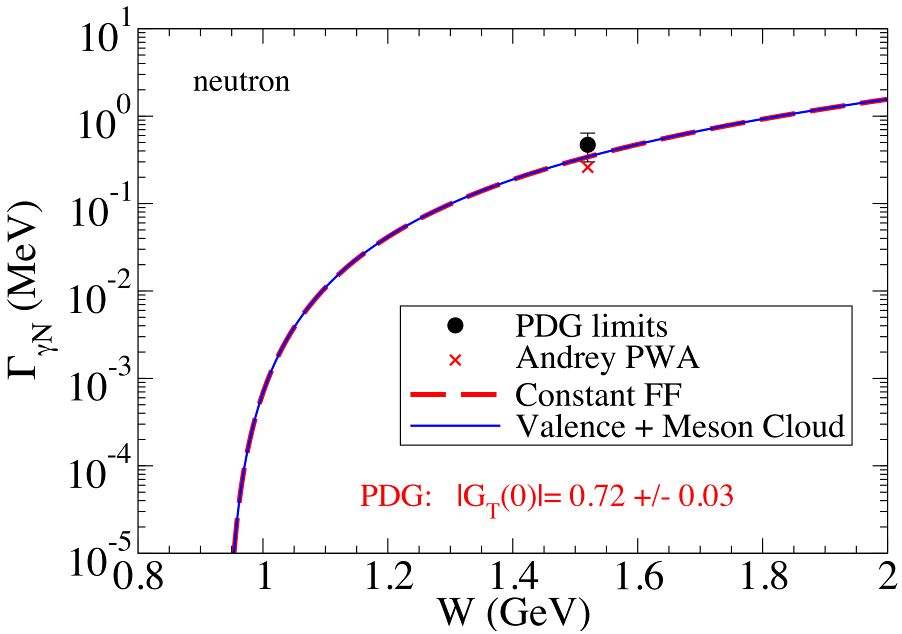

Devenish (1976) normalization of transition form factors

$$|G_T| \to \sqrt{\frac{2}{3}}|G_T|$$

$$G_T^{CST}(0, M_R) = 0.73$$

Consistent with PDG value for γN decay width.

Crossing the boundaries

N*(1520) Dalitz decay

2017 results

Neutron and Proton light dilepton decay width

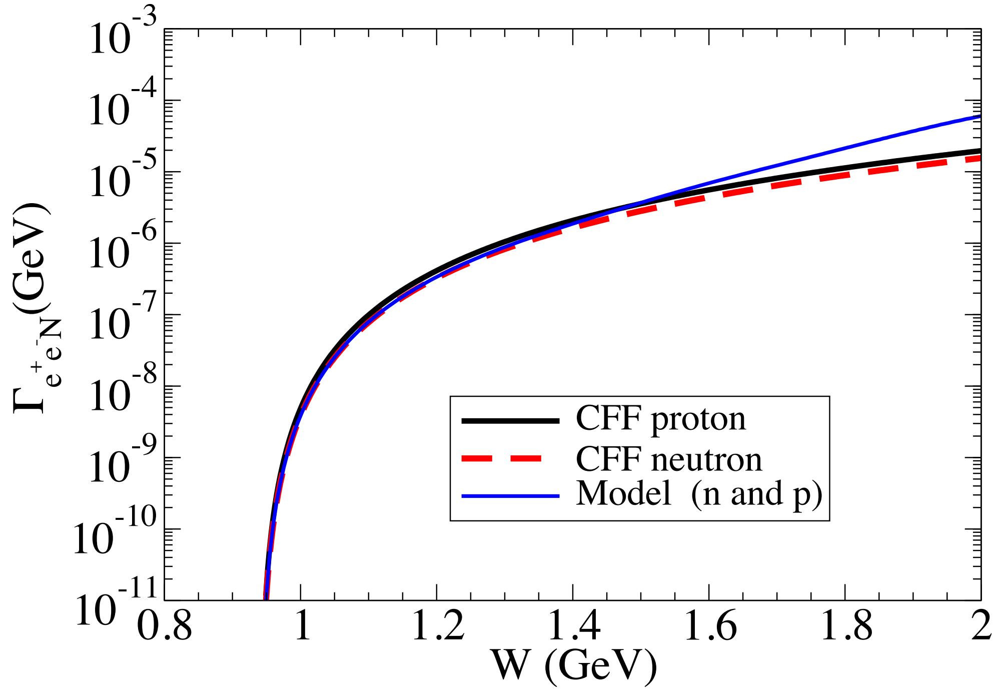

- Similar Proton and neutron results due to iso-vector dominance of meson cloud.
- At higher energies evolution of $G_T(q^2, W)$ with q^2 becomes important.

Crossing the boundaries

N*(1535)

Proton

Neutron

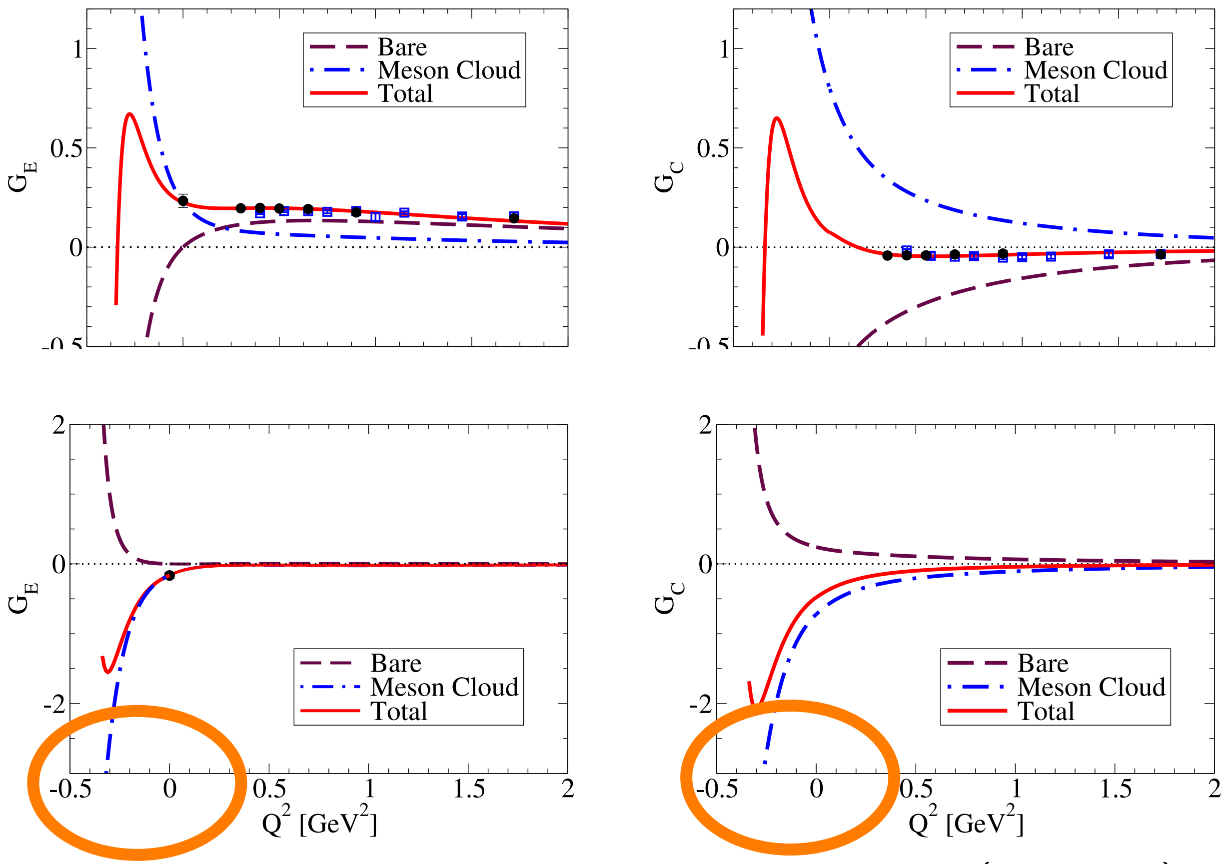

Analytic extrapolation to TL – Proton and neutron (real part)

In timelike it is preferable to use: $\eta = \frac{M_R - M_N}{M_R + M_N}$

$$G_E = F_1^* + \eta F_2^* \qquad\qquad G_C = -\frac{M_R}{2}\frac{M_R + M_N}{Q^2}\left[\eta F_1^* - \tau F_2^*\right]$$

Crossing the boundaries

N*(1535) Dalitz decay

$$\Gamma_{\gamma^* N}(q,W) = \frac{\alpha}{2W^3}\sqrt{y_+ y_-}\, y_+ B \| G_T(q^2,W)|^2,$$

$$|G_T(q^2,W)|^2 = |G_E(q^2,W)|^2 + \frac{q^2}{2W^2}|G_C(q^2,W)|^2$$

$$\frac{d\Gamma_{e^+e^-N}}{dq}(q,W) = \frac{2\alpha}{3\pi q^3}(2\mu^2+q^2)\sqrt{1-\frac{4\mu^2}{q^2}}\,\Gamma_{\gamma^* N}(q,W),$$

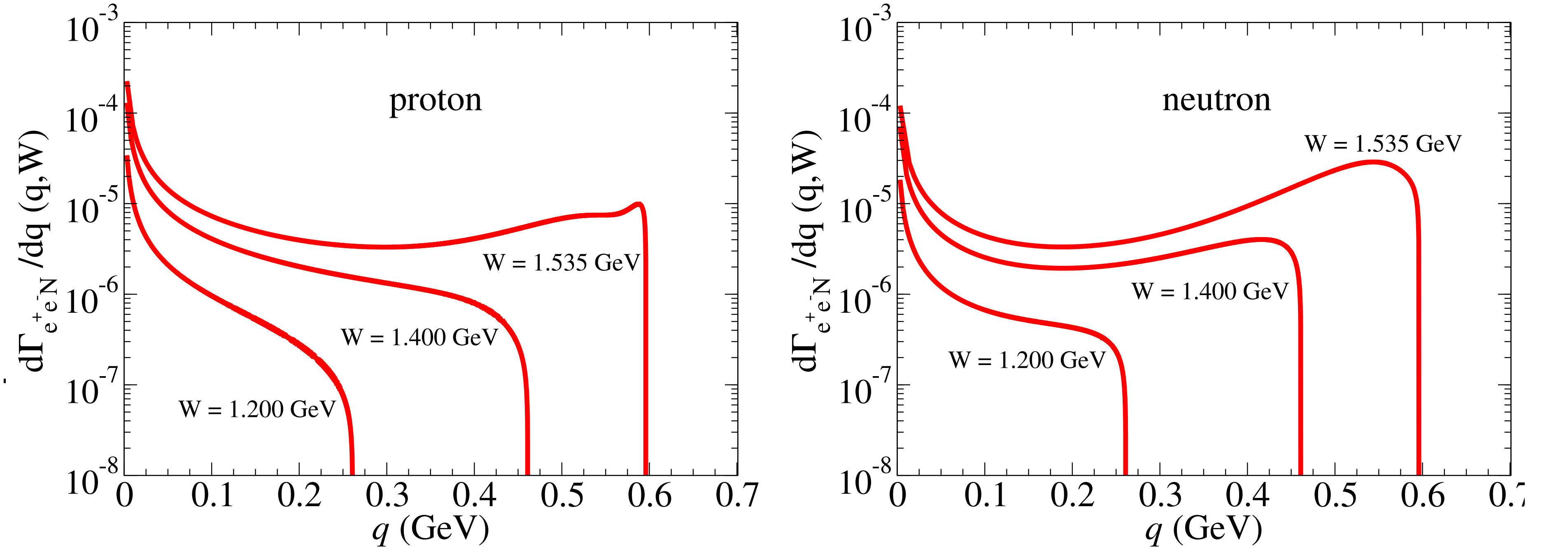

Crossing the boundaries N*(1535)

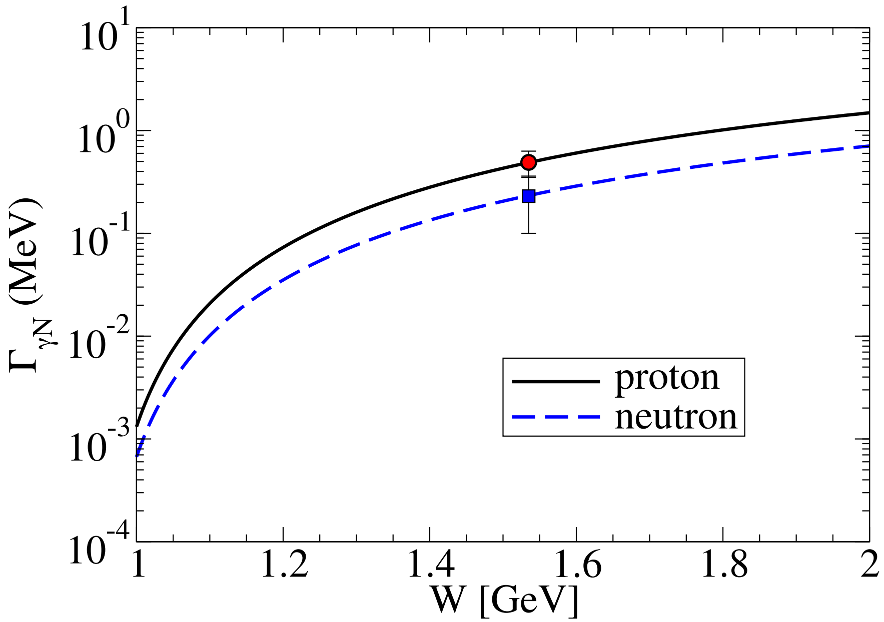

Electromagnetic decay

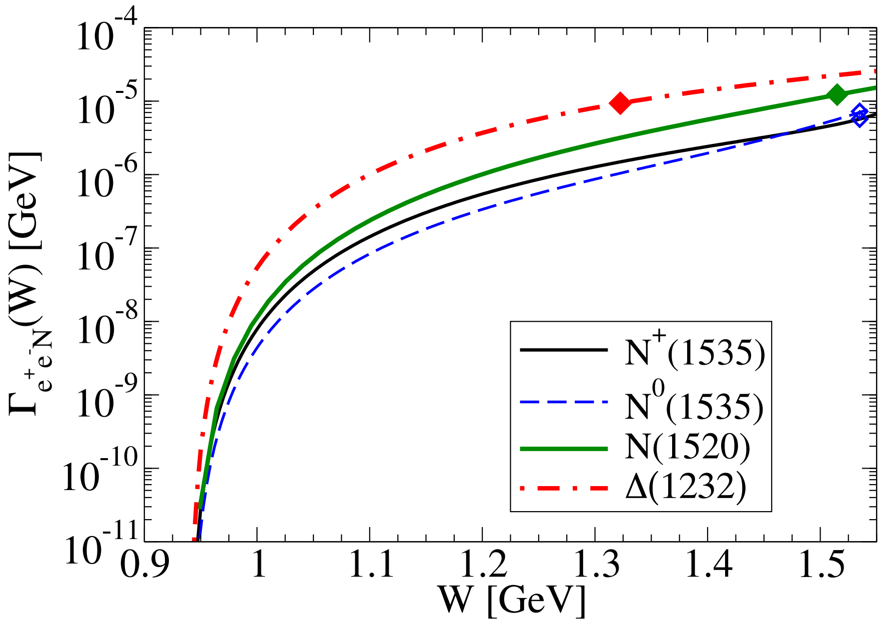

Dalitz decay (compared)

Different results for proton and neutron electromagnetic widths due to iso-scalar term in the meson cloud.

Dalitz decay widths similar for proton and neutron.

4. Some predictions for Hyperons

Extension to Strangeness

Timelike transitions appear as a
unique opportunity to explore hyperon structure.
N. Cabibbo and R. Gatto,
Phys. Rev. Lett. 4, 313 (1960);
Phys. Rev. 124, 1577 (1961).

They are new windows for the role of
diquarks in baryons, deduced from how form factors vary
with quark composition.
S. Dobbs, A. Tomaradze, T. Xiao,
K. K. Seth and G. Bonvicini,
Phys. Lett. B 739, 90 (2014)

Extension to Strangeness in the Spacelike region with a global fit to lattice data and physical magnetic moments

Extend the parametrization of the e.m. current to the valence quark d.o.f of the **whole** baryon octet.

$$j_i = \frac{1}{6} f_{i+} \lambda_0 + \frac{1}{2} f_{i-} \lambda_3 + \frac{1}{6} f_{i0} \lambda_s$$

$$\lambda_0 = \begin{pmatrix} 1 & 0 & 0 \\ 0 & 1 & 0 \\ 0 & 0 & 0 \end{pmatrix}, \qquad \lambda_3 = \begin{pmatrix} 1 & 0 & 0 \\ 0 & -1 & 0 \\ 0 & 0 & 0 \end{pmatrix}$$

$$\lambda_s \equiv \begin{pmatrix} 0 & 0 & 0 \\ 0 & 0 & 0 \\ 0 & 0 & -2 \end{pmatrix}$$

Parameters for valence quark degrees of freedom and the pion cloud dressing determined by a **global fit** to octet baryon lattice data for the e.m. form factors and physical magnetic moments.

Two examples:

Red line: lattice
Blue line: physical regime

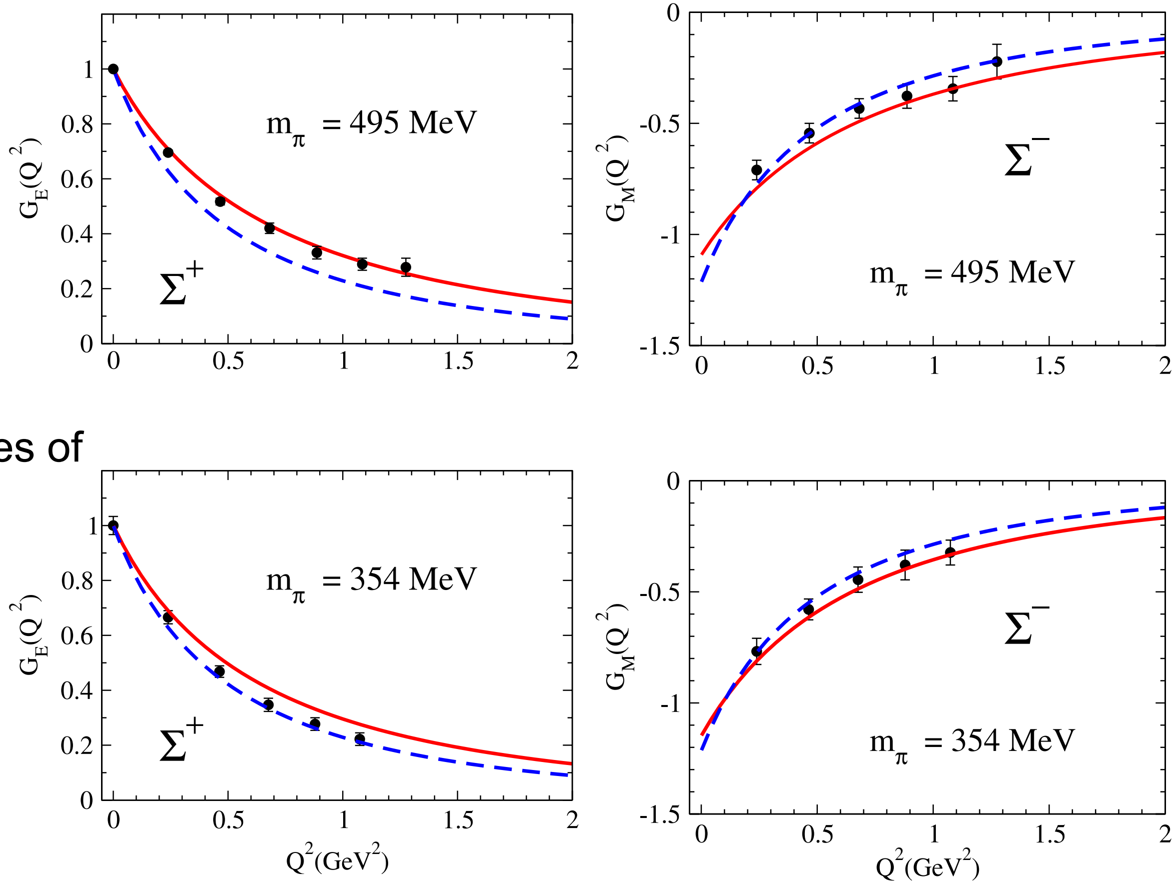

Lattice data:
H.W. Lin and K. Orginos, Phys. Rev. D 79, 074507 (2009).

G. Ramalho and K.Tsushima, PRD 84, 054014 (2011)

Extension to Strangeness in the timelike region

$$e^+e^- \to \gamma^* \to B\bar{B}$$

$$|G(q^2)|^2 = \left(1+\frac{1}{2\tau}\right)^{-1}\left[|G_M(q^2)|^2 + \frac{1}{2\tau}|G_E(q^2)|^2\right.$$
$$= \frac{2\tau|G_M(q^2)|^2 + |G_E(q^2)|^2}{2\tau+1}. \quad \tau = \frac{q^2}{4M_B^2}$$

Effective Form factor that gives the integrated cross section

Unitarity and Analiticity demand that for $q^2 \to \infty$

$$G_M(q^2) \simeq G_M^{\rm SL}(-q^2),$$
$$G_E(q^2) \simeq G_E^{\rm SL}(-q^2).$$

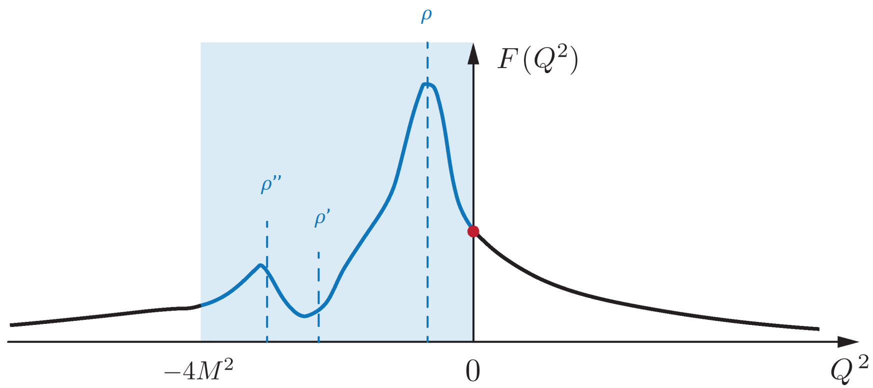

S.Pacetti, R. Baldini Ferroli and E. Tomasi-Gustafsson, Phys. Rept. 550-551,1 (2015)

CST seems to work well at large Q^2.

Extension to Strangeness in the timelike region

$$e^+e^- \to \gamma^* \to B\bar{B}$$

Data from
Babar,CLEO,BESIII

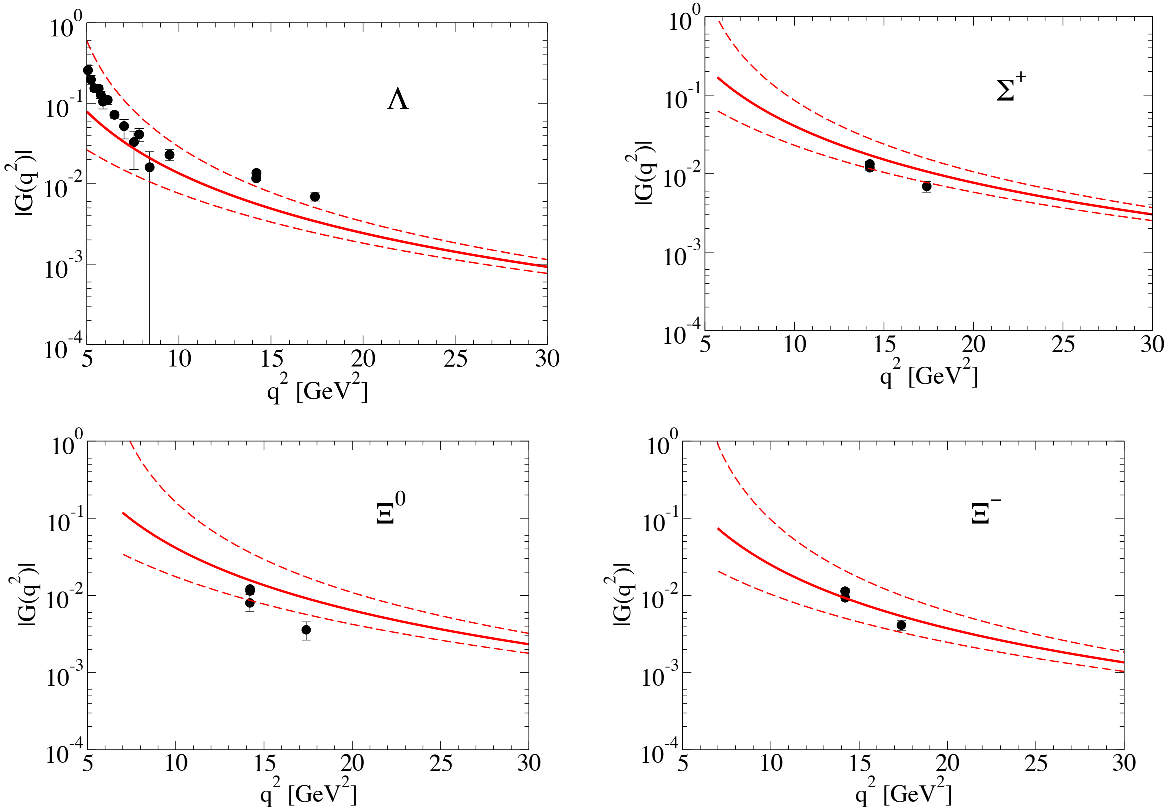

Full line: $G(q^2) = G(2M^2 - q^2)$

Dashed lines: $G(q^2) = G(4M^2 - q^2)$

$$G(q^2) = G(-q^2)$$

$$G_M(q^2) \simeq G_M^{\rm SL}(-q^2),$$
$$G_E(q^2) \simeq G_E^{\rm SL}(-q^2).$$

Extension to Strangeness in the timelike region

$e^+e^- \to \gamma^* \to B\bar{B}$

This enables:

- Predictions for future experiments

- Guidance for determination of onset of

-"reflection" symmetry validity

-perturbative QCD falloffs : $G_M \propto 1/q^4$ and $G_E \propto 1/q^4$.

Asymptotic behavior

$$e^+e^- \to \gamma^* \to B\bar{B}$$

Dominating term for large momentum tranfer

$$f_{1+} = \lambda + \frac{1-\lambda}{1+Q_0^2/m_v^2} + \frac{c_\pm Q_0^2/M_h^2}{\left(1+Q_0^2/M_h^2\right)^2}$$

$$f_{2\pm} = \kappa_\pm \left(\frac{d_\pm}{1+Q_0^2/m_v^2} + \frac{(1-d_\pm)}{1+Q_0^2/M_h^2} \right)$$

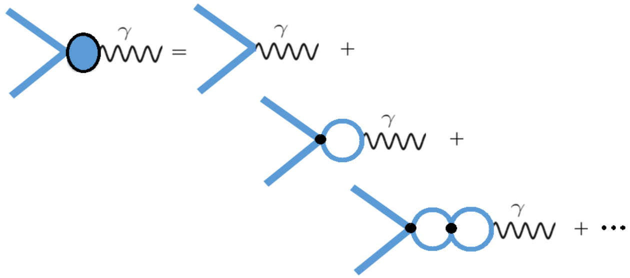

$$\Gamma_\mu(p,Q) = \quad \gamma_\mu \quad + \int \frac{d^4q}{(2\pi)^4} K(p,q,Q) S(q+\eta Q) \Gamma_\mu(q,Q) S(q-\eta Q)$$

Asymptotic behavior

$e^+e^- \to \gamma^* \to B\bar{B}$

Perturbative QCD limit is way above the region where refletion symmetry starts to be valid

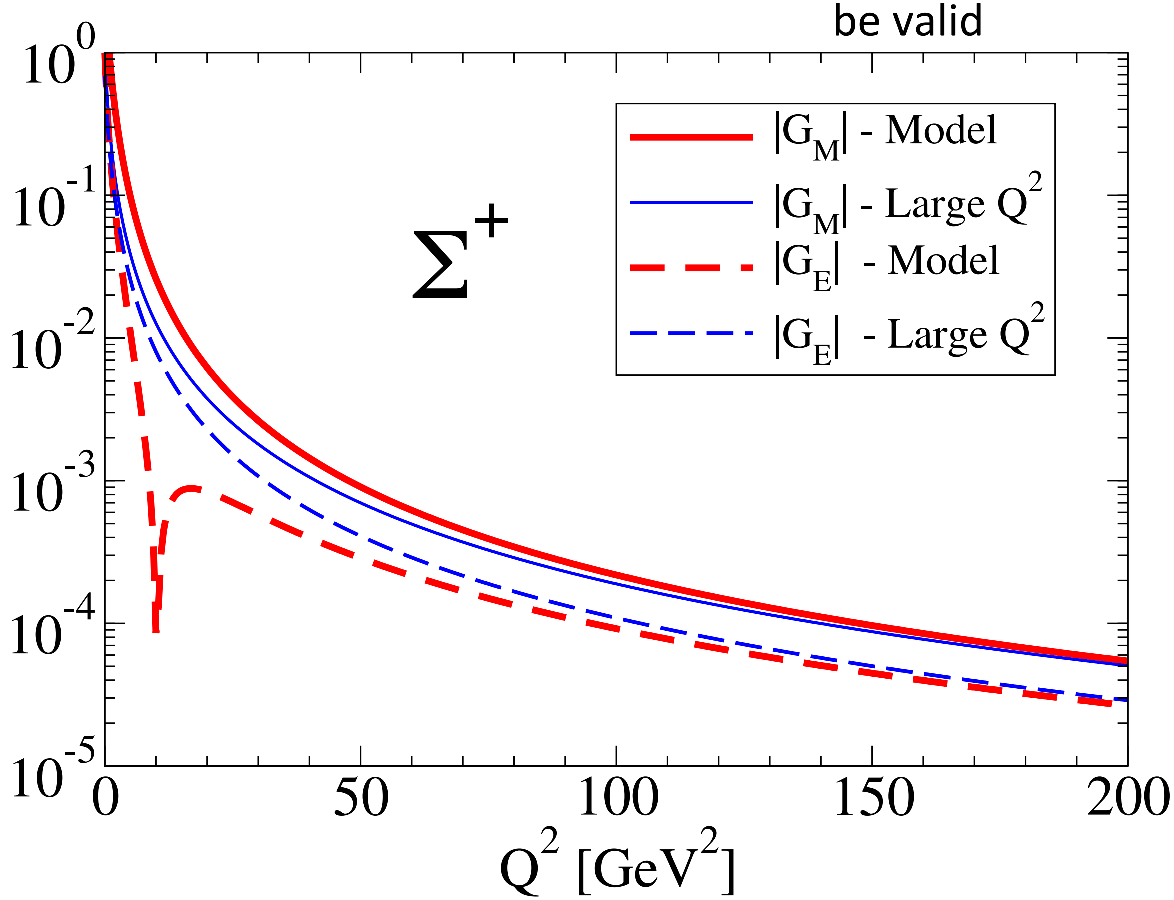

Summary

Covariant **S**pectator quark-diquark model enables description of different resonance states (spin/orbital motion).

Several applications: **Δ(1232)**, N*(1440), N*(1535)**, N*(1520)**,baryon octet, DIS, dilepton mass spectrum.

Consistent with experimental data at high Q^2.

Consistent with LQCD in the large pion mass regime informing on “pion cloud” effects, and **high q^2 behavior of time-like hyperon FFs**.

VMD and “pion cloud” sustained extension to the timelike region of the TFF of the **Δ(1232), N*(1520), N*(1535).**

Outlook

LQCD simulations below the N* threshold will help too refine interpretation provided by theoretical quark models.

LQCD data on the baryon octet e.m. FF's precious source of information, due to scarcity of experimental information.

New experimental data at large Q^2 and even more precise data in all ranges can improve interpretation of empirical results.

Dynamical calculations of diquark vertices within CST to be done, to support quark-diquark picture for baryons, seen within Dyson-Schwinger approach for dynamical quarks.

Thank you!

Alfred Stadler (Univ. Évora &IST-ULisboa)

Elmar Biernat (IST-ULisboa)

Gernot Eichmann (IST-ULisboa)

TÉCNICO LISBOA